AD-A119 175 STEVENS INST OF TECH HOBOKEN NJ OPTICAL COMMUNICATIO--ETC F/G 17/2
THE IMPACT OF DATA RATES ON THE DESIGN OF A FIBER OPTICS GUIDAN--ETC(U)
JUL 82 G J HERSKOWITZ DAAG29-81-D-0100
UNCLASSIFIED SOI-AD-E950 274 NL

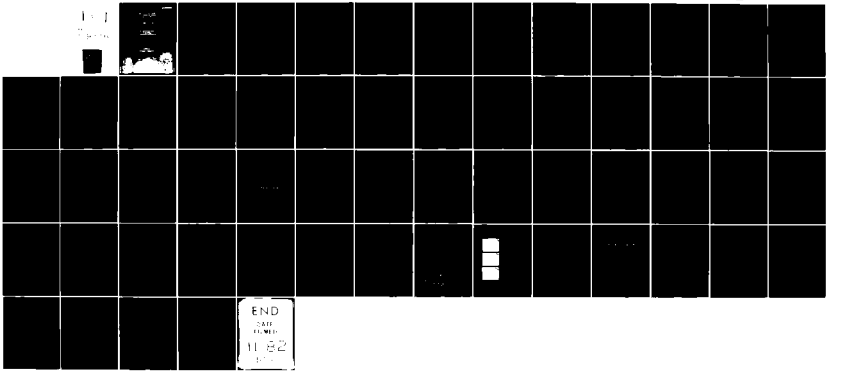

END
DATE FILMED
11-82
DTIC

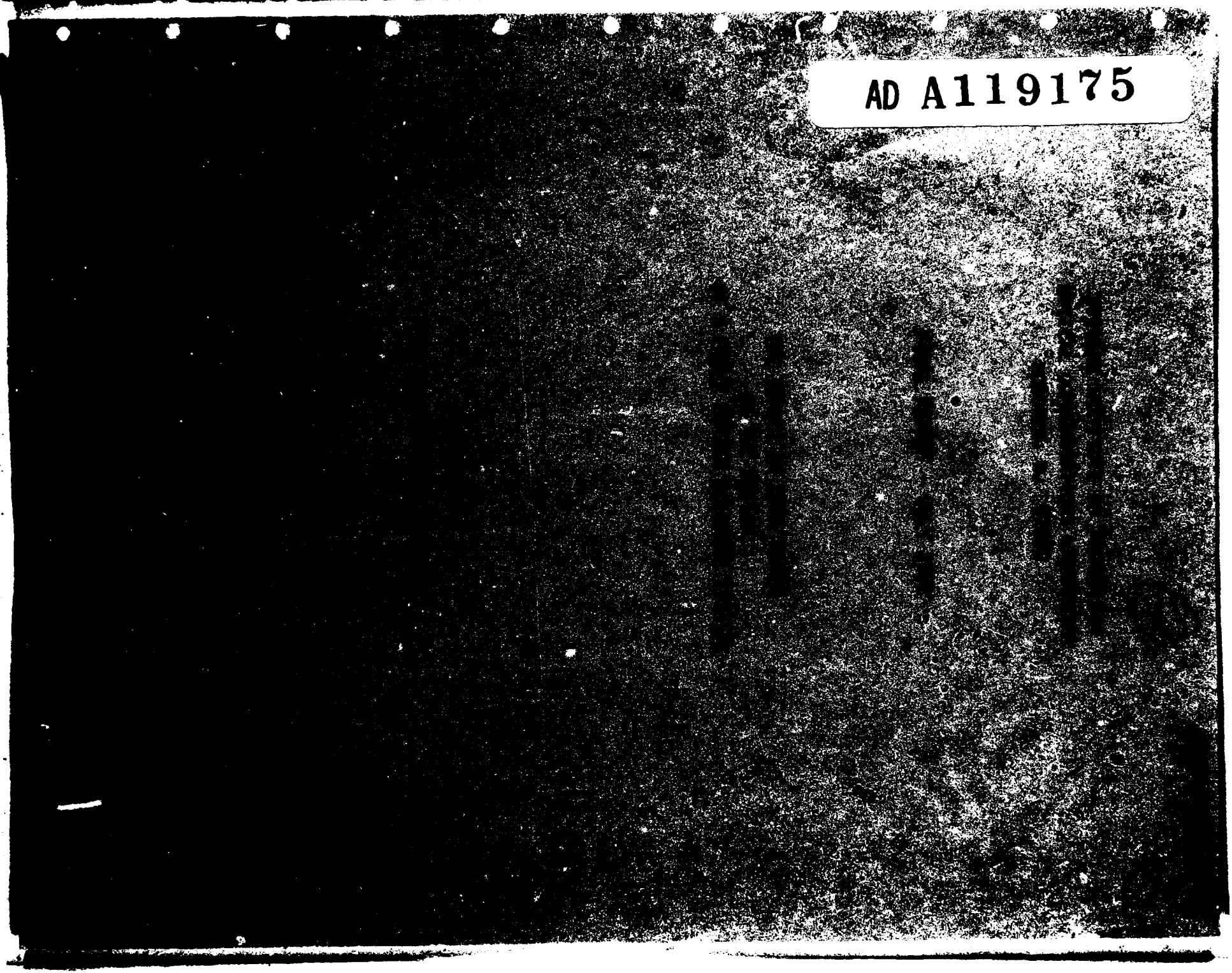

UNCLASSIFIED

SECURITY CLASSIFICATION OF THIS PAGE (When Data Entered)

REPORT DOCUMENTATION PAGE		READ INSTRUCTIONS BEFORE COMPLETING FORM
1. REPORT NUMBER	2. GOVT ACCESSION NO. AD-A119175	3. RECIPIENT'S CATALOG NUMBER
4. TITLE (and Subtitle) THE IMPACT OF DATA RATES ON THE DESIGN OF A FIBER OPTICS GUIDANCE SYSTEM.		5. TYPE OF REPORT & PERIOD COVERED FINAL REPORT February - June 1982
		6. PERFORMING ORG. REPORT NUMBER
7. AUTHOR(s) Dr. Gerald J. Herskowitz		8. CONTRACT OR GRANT NUMBER(s) DAAG29-81-D-0100 D.O. 0169 (TCN 82-022)
9. PERFORMING ORGANIZATION NAME AND ADDRESS Stevens Institute of Technology Optical Communications Laboratory Hoboken, NJ 07030		10. PROGRAM ELEMENT, PROJECT, TASK AREA & WORK UNIT NUMBERS 6.23.03.A - Prog. Element 1L162303A214 - DS Proj No. 612303.2140111.04 - AMCMS
11. CONTROLLING OFFICE NAME AND ADDRESS U.S. Army Research Office P.O. Box 12211 Research Triangle Park, NJ 27709		12. REPORT DATE July 1982
		13. NUMBER OF PAGES vi + 53 pp.
14. MONITORING AGENCY NAME & ADDRESS(if different from Controlling Office) U.S. Army Missile Command ATTN: DRSMI-RES Redstone Arsenal, AL 35898		15. SECURITY CLASS. (of this report) UNCLASSIFIED
		15a. DECLASSIFICATION/DOWNGRADING SCHEDULE

16. DISTRIBUTION STATEMENT (of this Report)

APPROVED FOR PUBLIC RELEASE; DISTRIBUTION UNLIMITED.

17. DISTRIBUTION STATEMENT (of the abstract entered in Block 20, if different from Report)

Same as 16.

18. SUPPLEMENTARY NOTES

19. KEY WORDS (Continue on reverse side if necessary and identify by block number)

Fiber Optics, Missile Guidance System, Data Rates

20. ABSTRACT (Continue on reverse side if necessary and identify by block number)

[SEE REVERSE SIDE.]

DD FORM 1 JAN 73 1473 EDITION OF 1 NOV 65 IS OBSOLETE S/N 0102-014-6601 |

UNCLASSIFIED

SECURITY CLASSIFICATION OF THIS PAGE (When Data Entered)

20. ABSTRACT

The data rate requirement of the optical fiber communication link for a missile guidance system has been evaluated. This data rate requirement is determined by the imaging seeker, sensors, and missile control system. The data rate limitations of the currently employed multimode optical fiber are determined for a specific signal-to-noise ratio using pulse frequency modulation. Available optical sources and detectors are evaluated, considering the effects of operating wavelength on fiber loss and dispersion characteristics. The effects of the fiber payout system on the fiber loss and dispersion characteristics are determined for both multimode and single-mode fiber. The use of optical multiplexing techniques to enhance fiber data rate is investigated. Recommendations are made for the most reliable, cost-effective approach for fiber optic missile guidance systems.

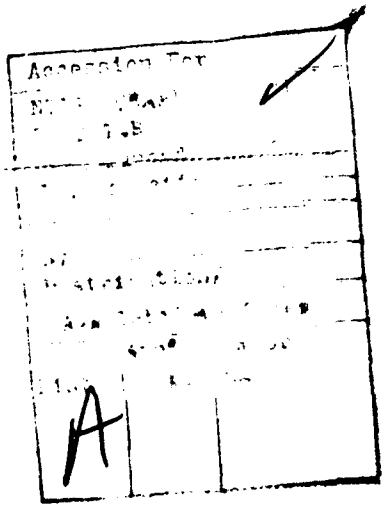

TABLE OF CONTENTS

THE IMPACT OF DATA RATES ON THE DESIGN OF A FIBER OPTICS GUIDANCE SYSTEM

1.0 BACKGROUND

A comprehensive concise summary of the developments leading to the successful FOG-D flight demonstration in September 1981 has been prepared by Mr. R. B. Powell.[1] It details the successful transmission of a standard 525 line daylight TV analog video signal to a ground station over a plastic-clad silica step-index optical fiber deployed from an attack RPV in early 1976. This was followed by a series of six missile flight tests utilizing the Ballistic Aerial Target Systems (BATS) between April and July 1977 which demonstrated the feasibility of transmitting unidirectional analog video signals over a fiber optic payout system at missile velocities and under missile operating conditions.

The High-Strength Payout Assembly developed by Hughes Aircraft and the full duplex data link designed by ITT/EOPD was funded by CORADCOM at the suggestion of CORADCOM. This work led to a FOG-D prototype link used in laboratory tests and simulation for the flight demonstration of a full-duplex data link, demonstrated in 1981.

Current plans for a ruggedized version of FOG-D, an Integrated Fiber Optic Communication Link (IFOCL), a FOG-M missile payout system, and an enhanced fiber optic guidance system have been summarized by Mr. H. Wichansky.[2] The recommendations and actions taken at this meeting relating to this study are:

a) Redirect the IFOCL program to address the FOG-M requirements. (See Table I.)

b) Expansion of the downlink capability to permit 6 additional telemetry channels through the use of electronically multiplexed frequency-shift keyed modulation of telemetry data.

c) Expansion of the video bandwidth from 5 to 10 MHz.

The data-rate requirements calculated in this study for television signals using pulse frequency modulation to achieve the 30 dB transmission signal-to-noise ratio (SNR), as specified in Table I for the IFOCL and FOG-M systems, are in the same range as the data rates required by typical infrared seeker signals after the thermal background level has been removed.[3]

TABLE I

CURRENT FIBER OPTIC COMMUNICATION LINK SPECIFICATIONS

	PRESENT GOALS (IFOCL)	REVISED (FOG-M)
VIDEO BANDWIDTH SNR	5 MHZ 30 dB	10 MHZ 30 dB
VIDEO FORMAT	525 LINES	SAME OR 875 LINES ADJUSTABLE
TELEMETRY	11 CHANNELS/60 HZ	SAME + 6 CHANNELS FSK (DATA RATE 100 Kb/s)
COMMAND	9 CHANNELS/60 HZ	SAME
PAYOUT VELOCITY	600 FT/S	SAME
MISSILE DIAMETER	6"	SAME
POWER	28 VDC	±5V ±15V

SOURCE: H. WICHANSKY

1.1 FIBER OPTIC GUIDED MISSILE COMMUNICATION SYSTEM DESCRIPTION

A general description of the fiber optic communication link, summarized from the information presented in a detailed paper,[4] will be used to provide a basis for the analyses presented in this report. Figure 1 illustrates the nature of signals in the bidirectional fiber optic link used in the guidance system. Information signals acquired by the missile sensors and seeker modulate the transmitter optical source after signal conditioning and encoding. The modulated sensor and video signals are transmitted from the airborne unit through a bidirectional coupler to the ground unit, where they are demodulated by the receiver, processed, and optically separated (demultiplexed) after passing through the ground station bidirectional coupler. Command signals, originating in the ground station, are electronically multiplexed and modulated optically in the transmitter for transmission through the bidirectional coupler and the optical fiber link to the missile. The current systems (IFOCL and FOG-M) under development employ a laser diode operating at 0.85 μm in the airborne unit transmitter and a 1.06 μm LED in the ground unit transmitter to achieve separation of the optical signals in the bidirectional link. These command signals are received and demultiplexed in the missile after transmission through the bidirectional coupler in the missile.

The video signals in the IFOCL and FOG-M systems use a conventional television camera with a 5 MHz bandwidth and 525 lines/frame for the IFOCL and 10 MHz with an adjustable number of lines/frame between 525 and 875 for FOG-M. Command and telemetry signals are either slowly varying analog or low data-rate digital data, as listed in Table I. Therefore, the bandwidth and data-rate requirements of the fiber optic link are determined primarily by the video signal. The sensor signals are multiplexed with the video signal, adding an insignificant bandwidth requirement to the link. Therefore, for the purpose of this analysis, only the video signal will be considered in determining the link data rate requirement.

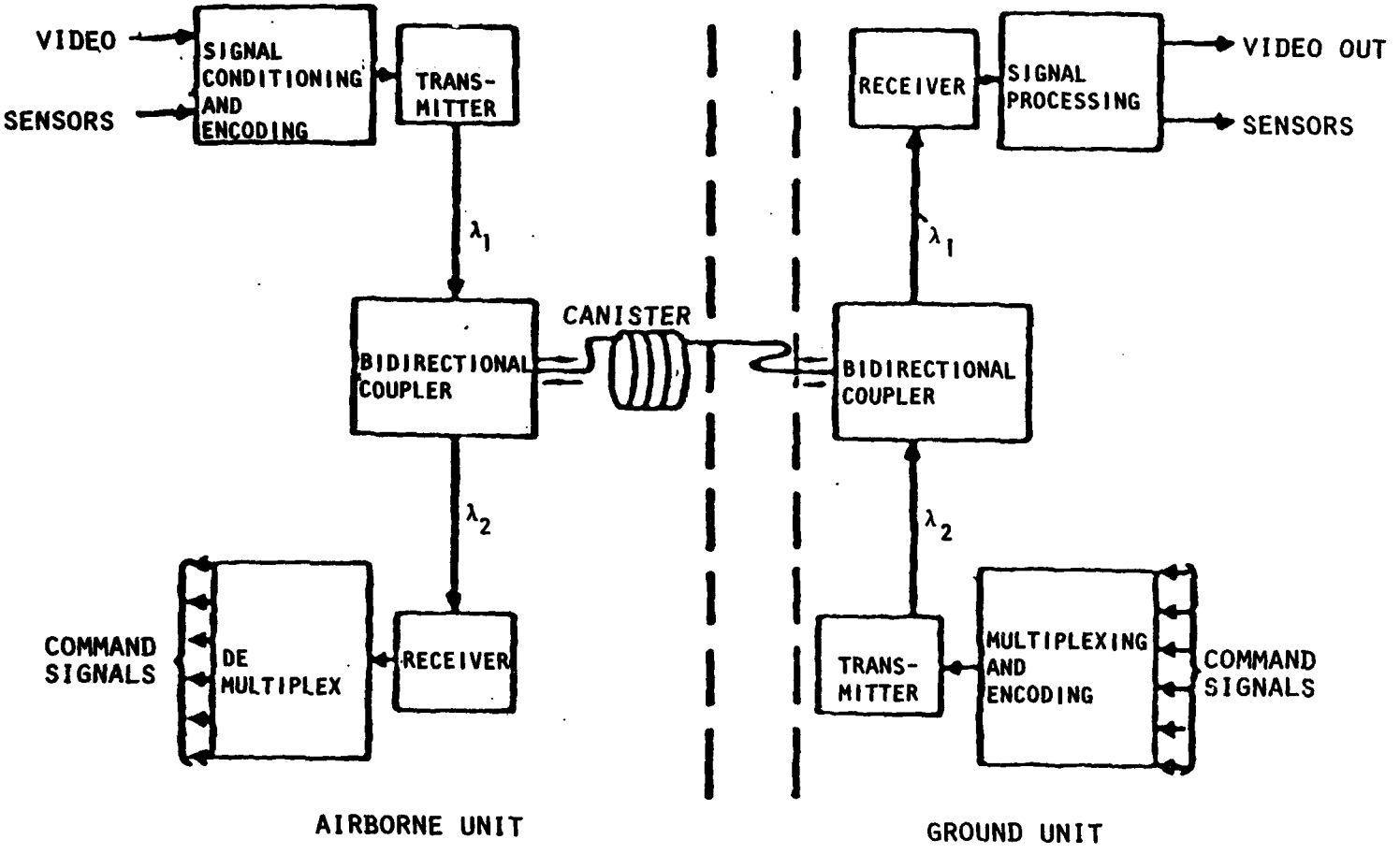

FIG. 1. FIBER OPTIC GUIDANCE LINK COMMUNICATION SYSTEM

2.0 IMAGE QUALITY DEPENDENCE ON FIBER OPTIC LINK DATA RATE, NOISE, AND OPTICAL SIGNAL MODULATION

Fidelity assessment in visual communications may be evaluated either by subjective testing or through the use of a distortion function.[5] A thorough study has been performed of the effects of video bandwidth, sensor resolution, sensor field of view, sensor video truncation, video frame rate, sensor control mode, and electronic zoom on Remotely Piloted Vehicles (RPV) operator tasks.[6] The RPV operator tasks which are significantly affected by these system parameters include: target search and detection, target recognition, sensor slew control, target designation and tracking, artillery burst detection and designation, and battle-damage assessment. Although the primary objective of this study was to determine the effects of bandwidth compression on operator performance of these tasks, the recommended RPV system design parameters summarized in Table II are useful as a subjective measure of image quality requirements.

In large part, these recommended parameter values are in agreement with current RPV system design, with the exception of the 0.075 frame/sec rate during target search and detection, compared with the 0.12 frame/sec current design value, used at the highest antijam level.

It is also recommended in this study that video truncation to achieve bandwidth compression could be used during target recognition, target designation, artillery burst designation, target tracking, and damage assessment operations. A video truncation of 8:1 is recommended when fields of view greater than 1.8 degrees are used. Note also that video zoom levels need to be determined for target and artillery burst designation, target tracking, and damage assessment.

The increased bandwidth capability of a fiber optic link may be employed to transmit more information to the ground unit, thus simplifying the electronics in the airborne unit. However, the distortion resulting from noise and bandwidth limitation due to the data rate capability of the fiber optic link must be determined before an evaluation of operator performance can be assessed. This requires the use of a distortion function, as described in Section 2.1.

TABLE II. OPERATOR TASKS AND RECOMMENDED RPV SYSTEM DESIGN PARAMETERS

Operator Task	System Design Parameter						
	Bandwidth Compression, Bits/Pixel	Sensor Resolution, TV Lines Across Target Height	Sensor Field Of View, Degrees	Video Truncation	Video Frame Rate, Frames/Second	Sensor Control Mode	Electronic Zoom
Target Search and Detection (Groups of Targets)	2	3	8.4 maximum	None	0.075 minimum	NA	None
Target Recognition	2	8	3.6 maximum	20:1 maximum	Frame update not required after first frame	NA	TBD
Sensor Pointing (Coarse Sensor Slew)	NA	NA	NA	None	2.0 minimum	No effect	None
Target and Artillery Burst Designation	NA	NA	NA	Field of view dependent. Up to 20:1 possible	2.0-4.0 minimum	Rate control	TBD
					0.075 minimum	Aided control	
Target Tracking	NA	NA	NA	Field of view dependent. Up to 20:1 possible	3.75 minimum	Rate control	TBD
Artillery Burst Detection	2	3	20	None	1.0 minimum	NA	None
Damage Assessment	2	8	1.8	8:1 maximum	Frame update not required after first frame	NA	TBD

Source: Reference 6

NOTE: N.A. = Not Applicable ; TBD = To Be Determined

2.1 DISTORTION OF VIDEO SIGNAL BY NOISE AND DATA-RATE LIMITATIONS

A measure of the distortion of the image received at the ground unit display due to fiber optic transmission system impairments such as data-rate limitations, noise, filter bandwidth restrictions, etc., may be obtained by using the rate-distortion function originally conceived by Shannon.[7] The rate distortion function of a signal source determines the minimum channel capacity required to transmit the source output as a function of the desired minimum average distortion, where the distortion function (sometimes called the fidelity criterion) is a measure of agreement between source and system output specified by the user. Shannon calculated the rate-distortion function for certain sources including, in particular, a Gaussian time-independent sample source.[8] This result was extended to continuous-time stationary processes by others.[9,10] These results have been applied to the transmission of images.[11-13]

The application of the rate-distortion function for the transmission of images may be formulated with the aid of Figure 2 which is a highly simplified communication system block diagram.

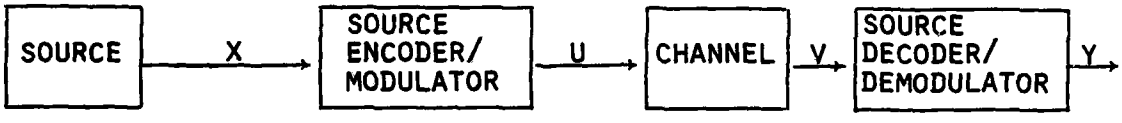

FIG. 2. RATE-DISTORTION MODEL

In the application of a fiber optic communication link to transmit images, the source is a seeker, either television video or an infrared imaging system. The source encoder consists of a signal processor (to remove redundancy) and a modulator which adds redundancy to improve the signal-to-noise ratio (SNR). The fiber optic link channel includes an optical source, bidirectional couplers, and the detector. The source decoder consists of a signal processor to restore the signal and a demodulator to recover the baseband signal.

The problem addressed by rate-distortion theory is the minimization of channel-capacity requirement while holding the average distortion at or below an acceptable level. To be specific, let the average information transmitted from the image source to the output in Figure 2 be denoted by the function $I(X,Y)$, defined as a measure of the amount of transmitted information. Also, let the average information transmitted from the encoder modulator to the channel output be denoted by $I(U,V)$. The channel capacity, C, is defined as the maximum of $I(U,V)$ over all possible image sources.

The large amount of available bandwidth in a fiber optic communciation system may be traded for improved SNR. Thus, the amount of redundancy removed by the encoding process in a fiber optic communication system is less than the redundancy added by the modulator to improve the SNR, and $I(U,V) \geq I(X,Y)$.

Since the channel capacity must be larger than the information transmitted over all possible image sources, $C \geq I(U,V)$. It has been established that it is always possible for $I(X,Y)$ to be arbitrarily close to C for an arbitrary source and channel structure.[12] The rate-distortion function $R(D)$ is the minimum value of $I(X,Y)$ for a given distortion level D, and it has also been established that $R(D) < C$ insures the possibility of obtaining distortion D.

Image distortion is caused by the fiber optic link in two ways: 1) a degradation of the SNR due to the noise introduced primarily by the optical source, detector, and receiver amplifier, and 2) distortion due to the data rate limitations of the optical fiber used in the link. Both of these causes of image distortion will be examined in detail.

2.2 TRANSMISSION OF TELEVISION SIGNALS IN BANDWIDTH-LIMITED CHANNEL WITH RANDOM NOISE

Results of subjective tests have led to direct evaluations of distortion caused by transmitting a television signal in bandwidth-limited noisy channels.[14] Although the fiber optic link has a wide bandwidth, there is a relationship between channel capacity C and SNR. For a channel in which the noise is Gaussian, this relationship has been shown to be:[7]

$$C = B \log_2(1 + \frac{S}{N}) \text{ bits/sec} \qquad (1)$$

where B is the channel bandwidth, S the signal power, and N is the total noise within the channel bandwidth B ($N=\eta B$ for a Gaussian channel, where η is the noise power spectral density).

The power spectrum of a television signal is illustrated in Fig. 3, along with typical noise characteristics.[15,16] Typically, the peak-to-peak signal to rms noise ratio from a good quality 625-line flying-spot scanner is of the order of 40 dB, with the source noise is, to all intents, Gaussian.[5]

The noise power may be independent of the signal amplitude, as in the vidicon camera, or it may increase with signal amplitude, as in the flying-spot scanner.[5] Noise added by an analog transmission channel will generally also be Gaussian, staying flat or rising with frequency, depending upon the modulation employed.

The Shannon-Hartley theorem of Eq.(1) indicates that a noiseless Gaussian channel (SNR = ∞) has an infinite capacity. However, the channel capacity does not become infinite as the bandwidth becomes infinite because with an increase in bandwidth, the noise power also increases. Thus, for a fixed signal power and in the presence of Gaussian noise, the channel capacity approaches an upper limit with increasing capacity, given by

$$\lim_{B \to \infty} C = 1.44 \frac{S}{\eta} \qquad (2)$$

known as the Shannon limit.

The Shannon-Hartley theorem indicates that for a particular modulation technique providing a capacity C, the bandwidth may be traded for SNR.

Or, alternatively, the capacity-increasing modulation technique may be used to increase the SNR for a fixed signal bandwidth. Examples of this principle are frequency modulation (FM) for analog signal and pulse code modulation (PCM) for digital signal transmission. The SNR of an FM system is increased by applying a large modulation index. Similarly, the probability of error, P_e in a PCM system is decreased by using a larger number of bits/sample to transmit the signal, thus increasing the amount of information in the channel, I(U,V) through the use of redundancy.

Channel bandwidth also affects television signal quality by producing a linear distortion which may be measured by a pulse and "bar" response.[5] The pulse has a sine-squared shape of 1/B width, where B is the channel bandwidth. The "bar" is a rectangular pulse some 25 μs in duration. The quality of the channel's response to rapid changes is tested by the pulse, while the flat top of the bar tests indicates how well the channel can keep to a constant value over a scanning line. The pulse and bar responses are checked against tolerance windows to establish the distortion of a television facility. The distortion level is measured for an average of transmitted television signals weighted for their deviation from the input. The measured weights are meant to be inverses of the relative visibilities of errors in reproduction and the distortion function is then equated to the most visible error.

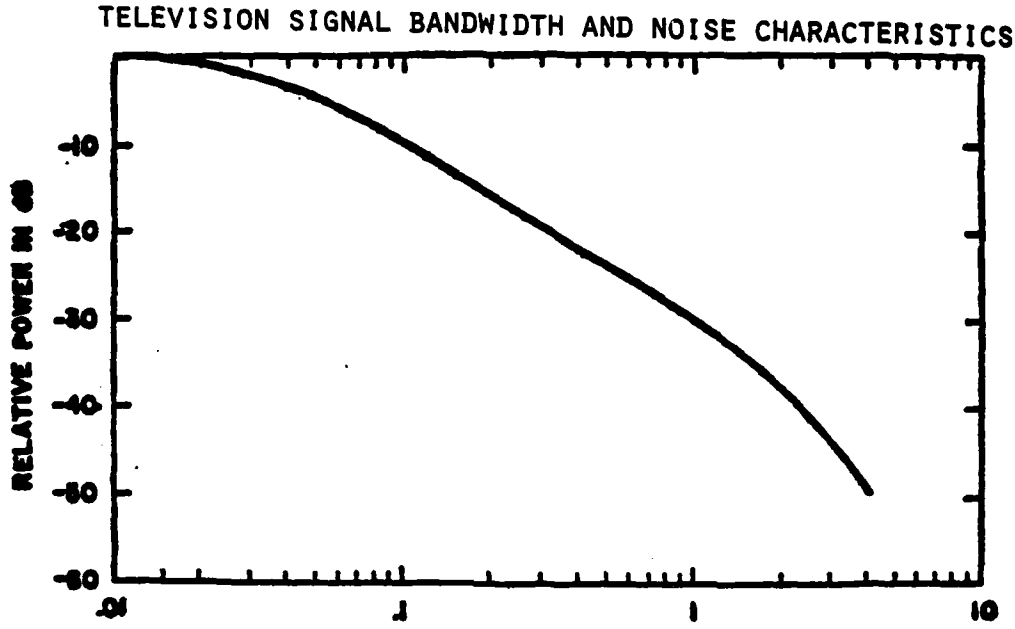

FIG.3a. POWER SPECTRUM OF VIDEO SIGNAL

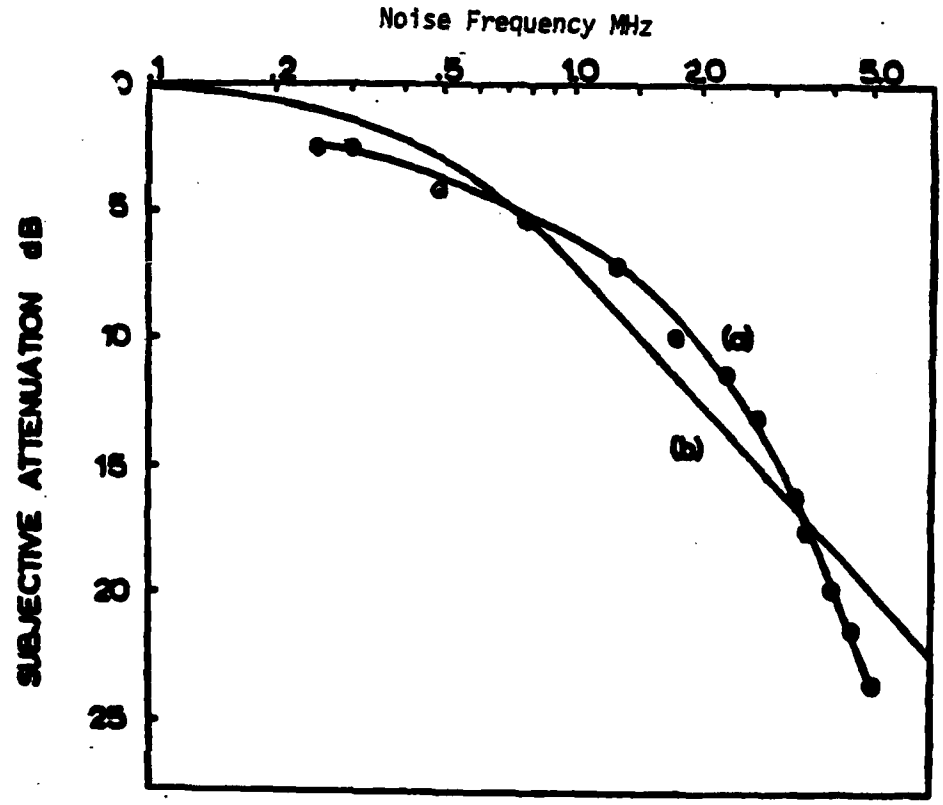

FIG.3b. NOISE WEIGHTING CHARACTERISTICS IN 625-LINE TELEVISION SYSTEM

SOURCE: Reference 15

(a) Measurements by Muller and Demus
(b) Standard CMTT Curve

2.3 DATA RATE REQUIRED TO TRANSMIT A TELEVISION IMAGE OVER A FIBER OPTIC LINK USING PULSE FREQUENCY MODULATION

Pulse frequency modulation (PFM) appears to be the most appropriate form of modulation for the transmission of television signals in a fiber optic link since it is particularly immune to the nonlinear distortion caused by optical source nonlinearities.[18] The PFM system shown in Figure 4 has been employed by the Naval Ocean Systems Center to transmit a composite television/data signal over an undersea fiber optic link.[19] The link exhibits a loss margin of nearly 60 dB for transmission of a 4.5 MHz bandwidth television signal, thus providing an unrepeated link span of 15 km with currently available optical fibers operating at a 0.85 μm wavelength. This link length does not include the effects of excess fiber loss due to the microbending losses caused by winding the fiber on a bobbin for high-speed payout.[20]

As in an FM communication system,[17] PFM may be used to increase the SNR at the expense of required channel bandwidth. This PFM "processing gain," $G^2 = \frac{(S/N)_o}{(C/N)_i}$ has been calculated to be:[19]

$$G = \frac{1.15\Delta F(1 + \Delta F^2/f_c^2)B}{f_c^{1/2} B_B^{3/2}} \quad , \tag{3}$$

where

$(C/N)_i$ = input pulse train power to noise power ratio in channel bandwidth,

$(S/N)_o$ = output signal power to noise power in baseband,

ΔF = maximum pulse train frequency deviation,

f_c = center frequency of pulse train,

B = fiber optic channel bandwidth,

B_B = baseband signal bandwidth assuming uniform signal and noise frequency spectral distributions.

The processing gain obtained by increasing ΔF relative to B_B in Eq.(3) may be understood by observing that the baseband signal is recovered by using a low-pass filter of bandwidth B_B following the discriminator (FM demodulator). Since the discriminator correlates the higher order FM signal components in the pulse train frequency range (vicinity

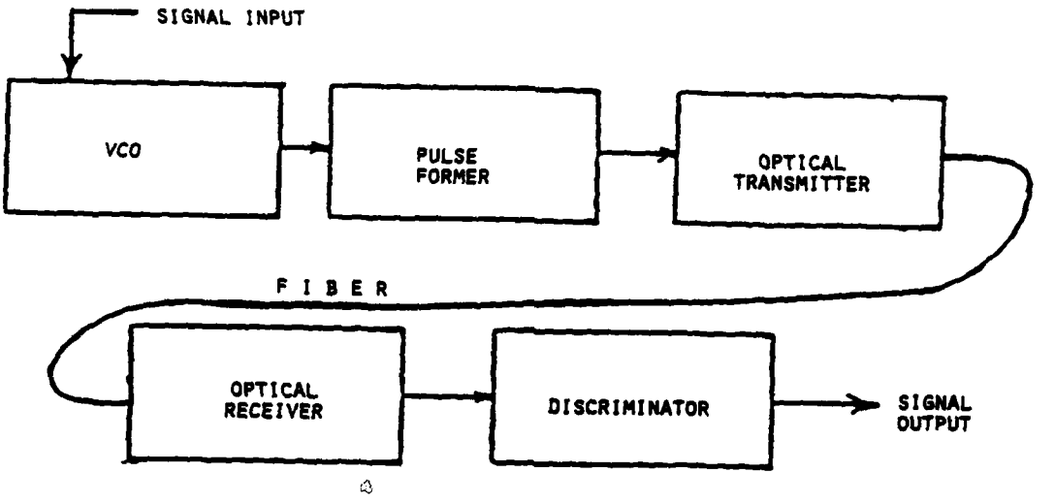

FIG. 4. PULSE FREQUENCY MODULATION SYSTEM

of f_c), the entire signal energy in this range is recovered. The random noise introduced at the imaging source, in the fiber optic link, and the receiver amplifier are attenuated out of the B_B band by the low-pass filter following the discriminator, resulting in the processing gain given by Eq.(3). The amount of processing gain is given in Table III for several values of $\frac{\Delta F}{B_B}$:

TABLE III

PROCESSING GAIN VS. $\frac{\Delta F}{B_B}$

$\frac{\Delta F}{B_B}$	20 log G
1	2.18
2	8.98
3	15.15
4	18.71
5	21.52

The maximum ratio of $\frac{\Delta F}{B}$ which can be used to achieve processing gain

depends on the bandwidth available in the fiber optic link and the threshold level required for the pulse-train power relative to the noise power at the output of the discriminator. This threshold level is analogous to the discriminator threshold of carrier to noise power in an FM system, below which noise "spikes" occur.[21] This FM threshold effect for values of $\Delta F/B_B$ = 0, 3, 12, are illustrated in Figure 5. Note that the threshold increases with the ratio $\Delta F/B_B$ and may be reduced by using a phase-locked loop (PLL) type of FM demodulator, which reduces the noise bandwidth.

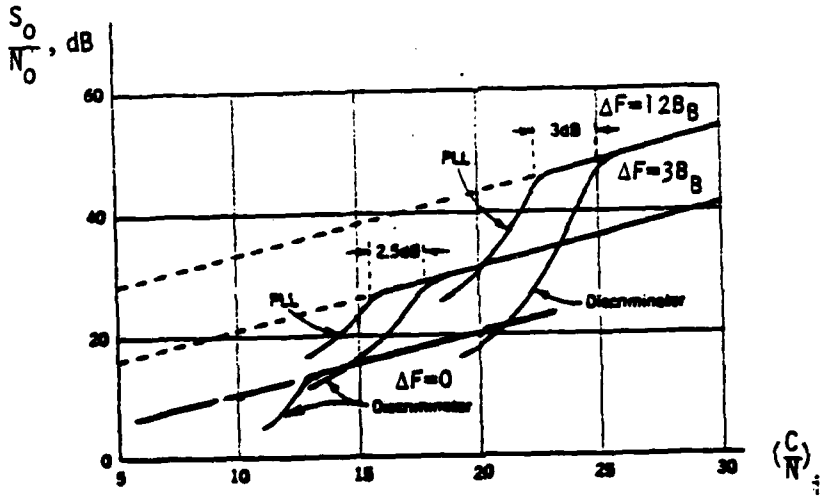

FIGURE 5.
THRESHOLD CHARACTERISTICS
OF DISCRIMINATOR/PHASE-LOCKED LOOP
FM DEMODULATORS

SOURCE: Taub and Schilling

The data rate required to transmit a television signal with a 30 dB SNR on a fiber optic link using PFM may be calculated by recognizing that there are three components in the out SNR, $(S/N)_o$, term:

1. The input pulse train carrier power, $(C/N)_i$, required to achieve the FM threshold of Figure 5.
2. The PFM processing gain given in Table III.
3. Pre-emphasis/de-emphasis filter gain.

A pre-emphasis/de-emphasis set of filters are generally employed in an FM system to overcome the parabolic increase with frequency of noise by an FM modulator.[17] The pre-emphasis filter increases the high-frequency content of signal level before modulation, and the de-emphasis filter reduces it accordingly to produce a SNR gain of about 6 dB.

As may be observed from Figure 5, the $(C/N)_i$ threshold required for a frequency deviation, ΔF, of about $2B_B$ is approximately 15 dB using a phase-locked loop (PLL) demodulator. Therefore, the required 30 dB SNR may be achieved according to the following contributions:

$(C/N)_i$ Threshold	15 dB
PFM Processing Gain ($\Delta F = 2B_B$)	9 dB
Pre-Emphasis/De-Emphasis Filter Gain	6 dB
REQUIRED $(S/N)_o$	30 dB

The optical fiber bandwidth required to sustain a pulse train frequency deviation $\Delta F=2B_B$ may be estimated from Carson's rule for an FM system:[17]

$$B \approx 2(B_B + \Delta F) = 6\ B_B \qquad (4)$$

However, in a PFM system, the data rate required to transmit pulses at this frequency depends upon the pulse response of the optical fiber. In an optical fiber of bandwidth B, the output pulse displays a temporal variation which may be approximated by a Gaussian response with a pulse width at the 1/e points defined as τ_e:

$$\tau_e = 2\sqrt{2}\,\sigma \quad , \qquad (5)$$

where σ is the rms Gaussian pulse width.[22] The 3 dB electrical bandwidth may be expressed in terms of τ_e as:

$$f(3\text{ dB elec.}) = \frac{0.375}{\tau_e}\ \text{Hz} \quad , \qquad (6)$$

which will be used as the definition of channel bandwidth B.

The data rate required to transmit pulses at the frequency specified by Carson's rule in Eq.(4) depends upon the allowable detector threshold penalty due to intersymbol interference caused by the overlap of the Gaussian pulse "tail" with the succeeding pulse.[22] This intersymbol interference (ISI) penalty will increase the power required by the transmitter for a particular fiber length. A plot of ISI power penalty in dB as a function of the ratio of τ_e to the bit-rate interval T is given in Figure 6. It demonstrates that the ISI power penalty is relatively small until the ratio τ_e/T exceeds 0.5. The data rate is equal to $1/T$.

Therefore, the relationship between data rate and bandwidth for an optical fiber may be obtained by selecting an allowable ISI penalty and then calculating the value of $1/T$ which will limit this ISI penalty for a particular value of τ_e, which is then related to bandwidth B through Equation (6):

$$\frac{1}{T} = 2.67B\left(\frac{\tau_e}{T}\right)_{ISI} \quad \frac{\text{Bits}}{\text{Sec}} \quad , \tag{7}$$

where $\left(\frac{\tau_e}{T}\right)_{ISI}$ is the power penalty resulting from the ratio of $\frac{\tau_e}{T}$, given in Figure 6. Therefore, if $\frac{\tau_e}{T} \leq 0.5$, for $\Delta F = 2B_B$, using Carson's rule in Eq.(4), the required data rate is 8.01 B_B bits/sec. Note that as τ_e increases due to fiber dispersion, as described in Section 3, the required data rate increases for an acceptable ISI power penalty.

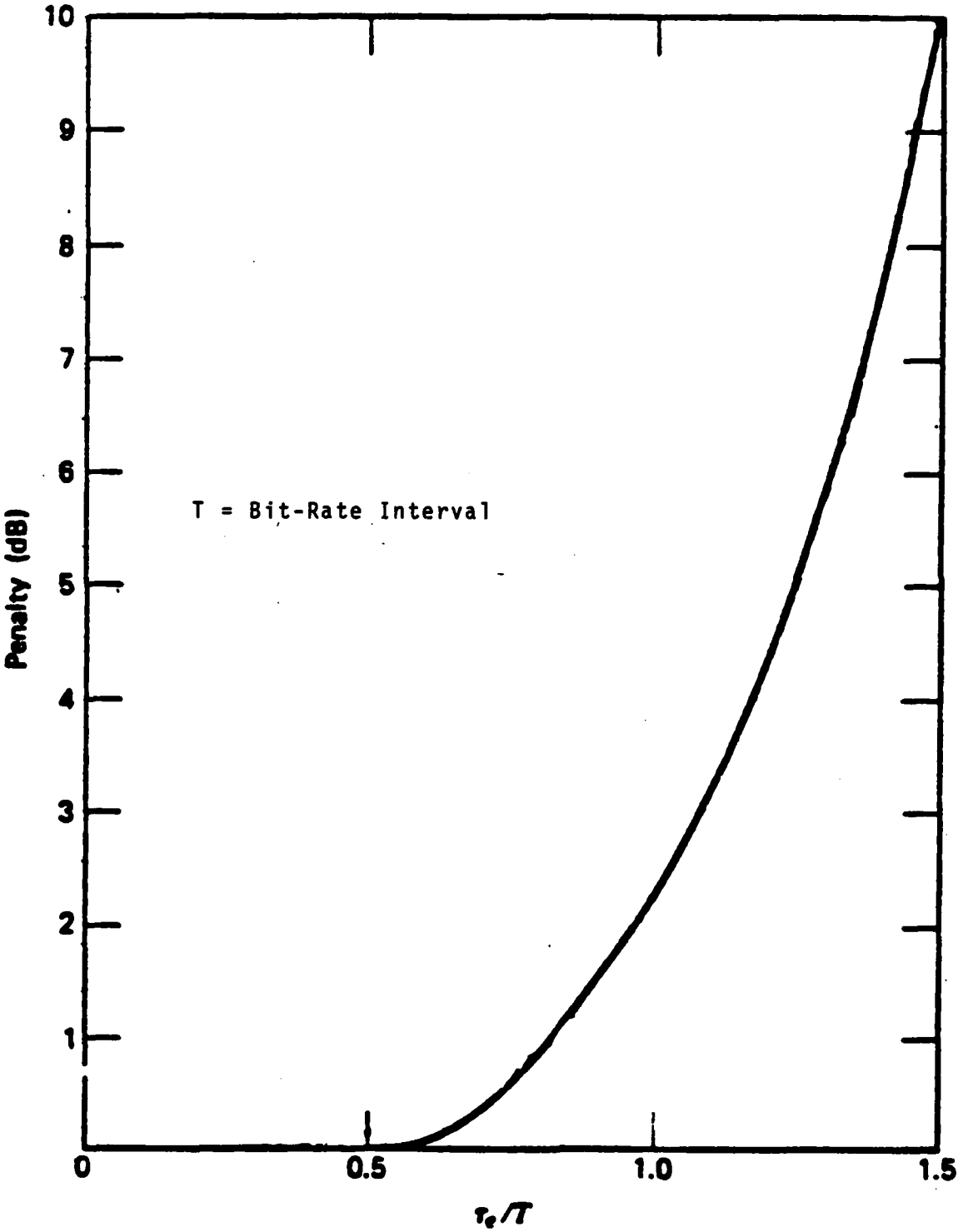

FIG. 6. INTERSYMBOL INTERFERENCE LOSS PENALTY

3.0 DATA RATE AND LENGTH LIMITATIONS IMPOSED ON FIBER OPTIC LINK BY OPTICAL FIBER DISPERSION AND ATTENUATION CHARACTERISTICS

The dispersion and loss characteristics of optic fibers determine the data rate and range limitations of the fiber optic link. These characteristics are reviewed in this section.

3.1 FIBER DISPERSION IN MULTIMODE AND SINGLE-MODE OPTICAL FIBERS

The relationship between data rate, signal bandwidth, and ISI power penalty, developed in Section 2.3 for a PFM system applies generally in a fiber optic link, through Eq.(7), for any modulation employed in the link. The increase in required data rate due to optical fiber dispersion is reflected in the factor $(\tau_e/T)_{ISI}$. For a particular value of τ_e, the allowable ISI power penalty determines the required data rate. The value of τ_e is increased through optical fiber dispersion according to the relationship:[22]

$$\tau_e^2 = (0.408T)^2 + (\phi_M \Delta\lambda L)^2 \pm (\psi L^b)^2 , \qquad (8)$$

where

ϕ_M = material dispersion factor,

$\Delta\lambda$ = maximum spectral width due to source and signal modulation bandwidth,

L = optical fiber length,

ψ = modal dispersion factor,

$1 \geq b \geq \frac{1}{2}$, depending on mode coupling effects.

The first term of Eq.(8) originates from the relationship between the rms Gaussian pulse width, σ, given by Eq.(5) in terms of τ_e, and the transmission of a rectangular pulse of width T/2. The received rms pulse width, σ, is defined as

$$\sigma^2 = \int_{-\infty}^{\infty} t^2 h(t)dt - \left[\int_{-\infty}^{\infty} t\, h(t)dt\right]^2 \qquad (9)$$

where $\int_{-\infty}^{\infty} h(t)dt = 1$ defines the pulse shape. Using this relationship, the T/2 rectangular pulse corresponds to an rms pulse width of $T/\sqrt{48}$ and $\tau_e = 2\sqrt{2}\,\sigma = 0.408T$, the first term of Eq.(8).

The second term of Eq.(8), describing the effects of material

dispersion on pulse width, is caused by chromatic effects, i.e., the combined effects of material and waveguide dispersion. The cause of chromatic dispersion is the wavelength dependence of the mode group velocity, v_g, due to the dependence of the index of refraction, n, on wavelength λ. The pulse spreading Δt over a fiber of length L is

$$\frac{\Delta t}{L} = \frac{1}{v_g} = \frac{\lambda^2}{c} \frac{\Delta \lambda}{\lambda} \cdot \frac{d^2 n}{d\lambda^2} \qquad (10)$$

where c is the speed of light.[23]

The second derivative of the refractive index n with respect to wavelength λ is characteristic of glass.[23] It has been determined that for pure silica a "zero material dispersion" (ZMD) point occurs at $\lambda = 1.27$ μm.[24] Adding various dopants to the silica glass can shift the ZMD point somewhere within the 1.2-1.4 um range, thereby allowing a very small increase in τ_e, particularly in single-mode fibers, as illustrated in Figure 7 for an 11 kilometer single-mode fiber.

In multimode fibers, dispersion is dominated by the difference in group velocity between various propagating modes and the wavelength dependence of the group delay for each mode, as expressed by Eq.(10). A simple ray analysis demonstrates a time difference Δt between the fastest (low angle of propagation) and the slowest (maximum angle of propagation) in a fiber of length L :

$$\frac{\Delta t}{L} \approx (NA)^2 / 2 n_c c \qquad (11)$$

where $NA = \sin\theta_{max}$, fiber numerical aperture,

n_c = fiber core index of refraction

For fibers where mode mixing is substantial (graded-index fibers and mode mixing due to microbending effects), it is found that the pulse spreading dependence is closer to $\sqrt{L}$ rather than L, giving rise to the factor b in Eq.(8), where $1 \geq b \geq \frac{1}{2}$, as demonstrated in Figure 8 for the Bell FT3 Lightwave System.[25]

The dispersion due to multimode effects may be minimized at a particular wavelength by optimizing the grading profile α in the fiber

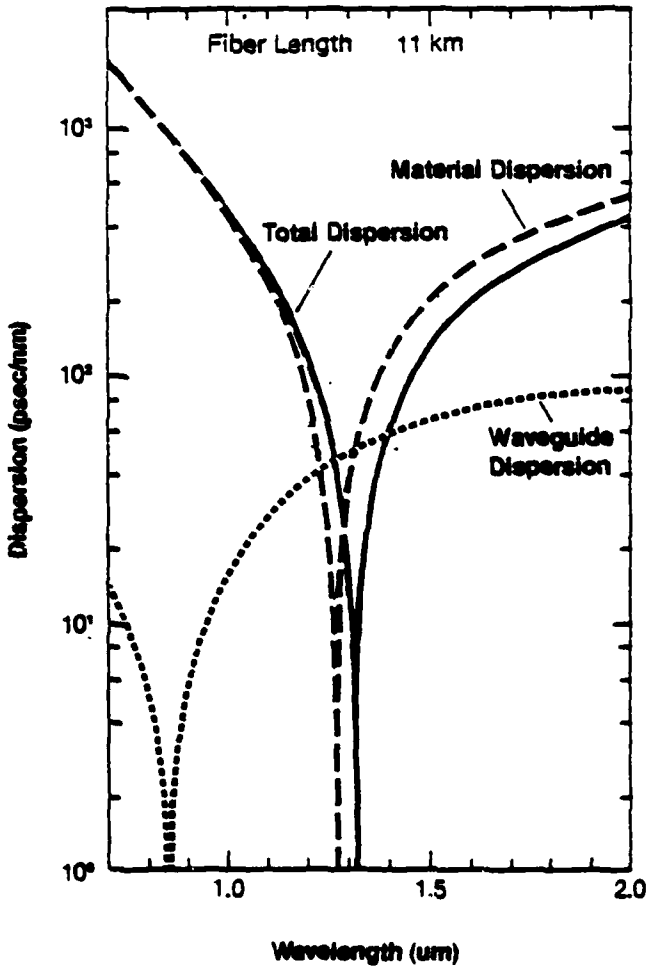

FIG. 7. DISPERSION IN SINGLE-MODE FIBER

SOURCE: Reference 24

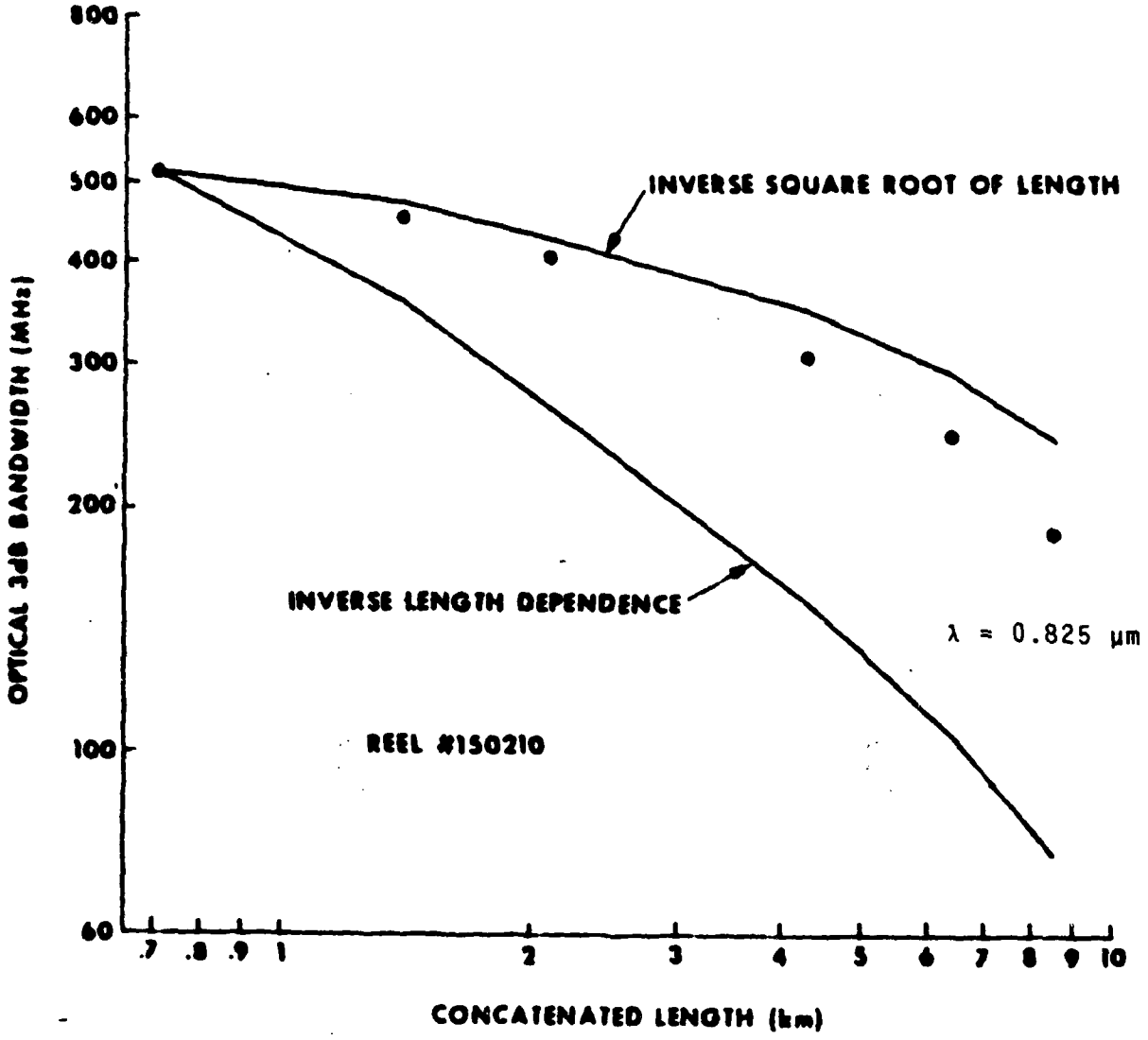

FIG. 8. GRADED INDEX MULTIMODE FIBER BANDWIDTH
BELL SYSTEM FT3 LIGHTWAVE SYSTEM

SOURCE: BELL TELEPHONE LABORATORIES (Ref.25)

core refractive index profile, described as a function of radius r :[26]

$$n(r) = n_1^2[1 - 2\Delta(\lambda)(r/a)^{\alpha}] \quad , \tag{12}$$

where

n_1 = maximum refractive index at the center of the core

$\Delta(\lambda) = [n_1^2 - n^2(a)]/2n_1^2$,

a = core radius .

The optimum value of α is given by:[26]

$$\alpha_{opt}(\lambda) = 2[1 - \frac{6}{5} P(\lambda)\Delta\lambda] \quad , \tag{13}$$

where

$$P(\lambda) = \frac{n_1}{N_1} \frac{\lambda}{\Delta} \frac{d\Delta}{d\lambda} \quad ,$$

$$N_1 = n_1 - \lambda \, dn_1/d\lambda \quad .$$

Note that the optimum value of α is a function of wavelength λ . Therefore, the bandwidth may be maximized at a particular value of λ , as demonstrated in Figure 9. Note that a large bandwidth may be achieved over a broader range of wavelengths (at a slight decrease in the maximum) by converting two fibers with different optimum values of α (1.8 and 2.014). This principle has been studied recently to enhance fiber bandwidth by connecting fibers of different values of α(opt.) to maximize overall bandwidth.[27,28]

3.2 FIBER LOSSES IN MULTIMODE AND SINGLE-MODE OPTICAL FIBERS

Intrinsic optical fiber loss mechanisms, illustrated in Figure 10, are caused by Rayleigh scattering loss, hydroxyl ion loss, and absorption at the ultraviolet and infrared wavelengths.[29] In addition to these losses, the missile fiber optic link sustains spooling losses, demonstrated by the measurements shown in Figures 11 and 12 for typical optical fibers tested for this purpose.[30] The primary source of intrinsic loss is Rayleigh scattering, which decreases with wavelength at a rate proportional to λ^{-4}, making operation of the fiber optic link at the longer wavelengths shown in Figure 10 very attractive. A more detailed description of the spooling losses and how they relate to fiber bandwidth will be developed in Section 4 of this report.

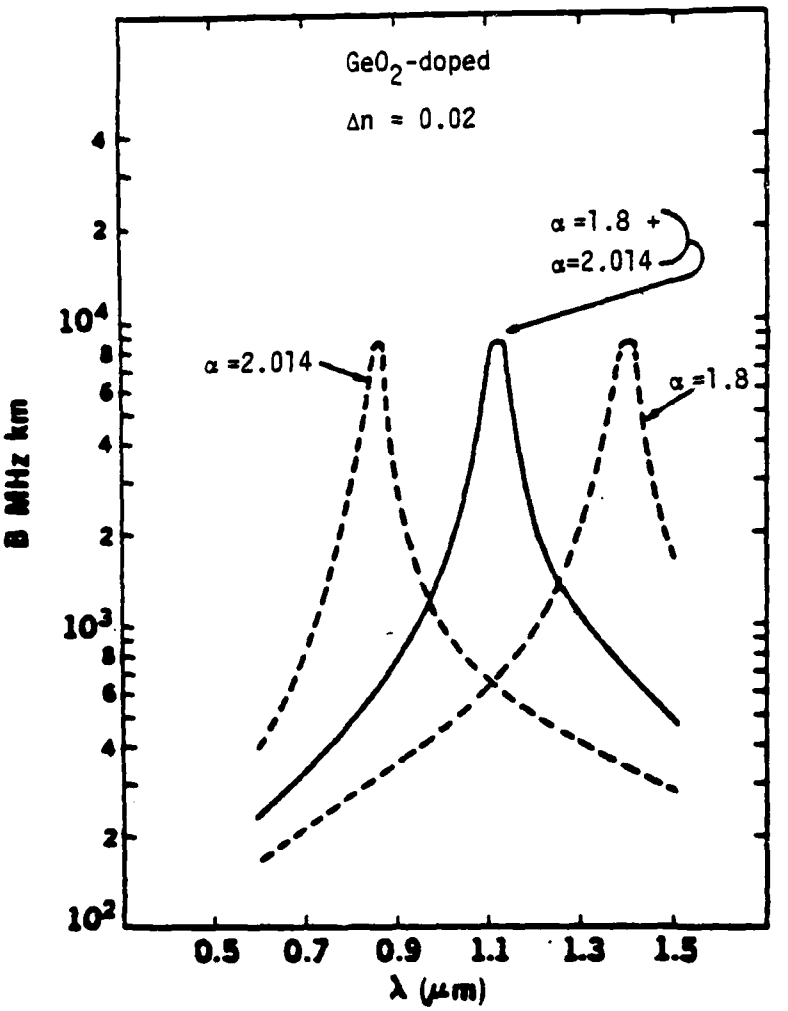

FIG. 9. EFFECT OF INDEX GRADING AND WAVELENGTH ON MULTIMODE FIBER BANDWIDTH

SOURCE: Reference 26

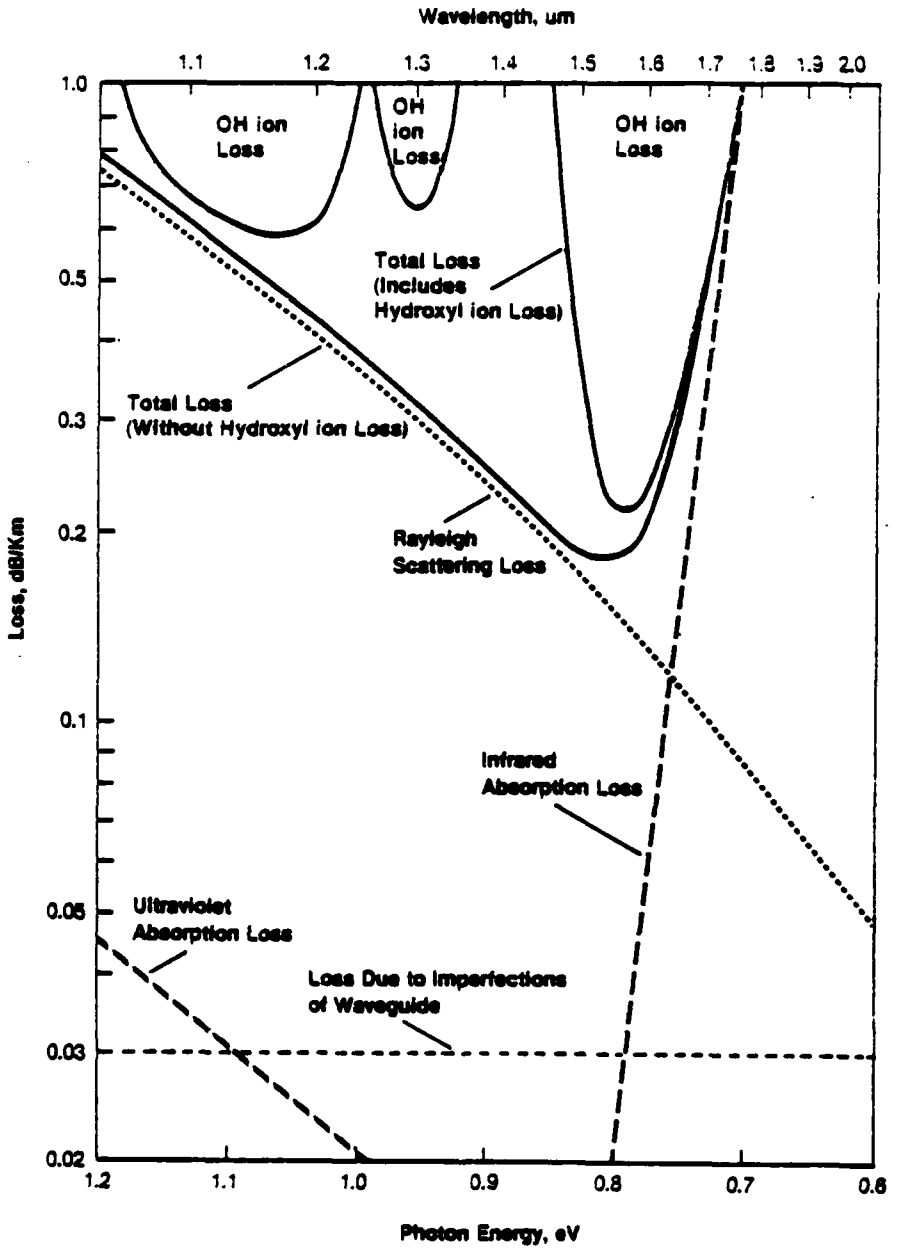

FIG. 10. INTRINSIC LOSS MECHANISMS IN OPTICAL FIBERS

Source: Reference 29

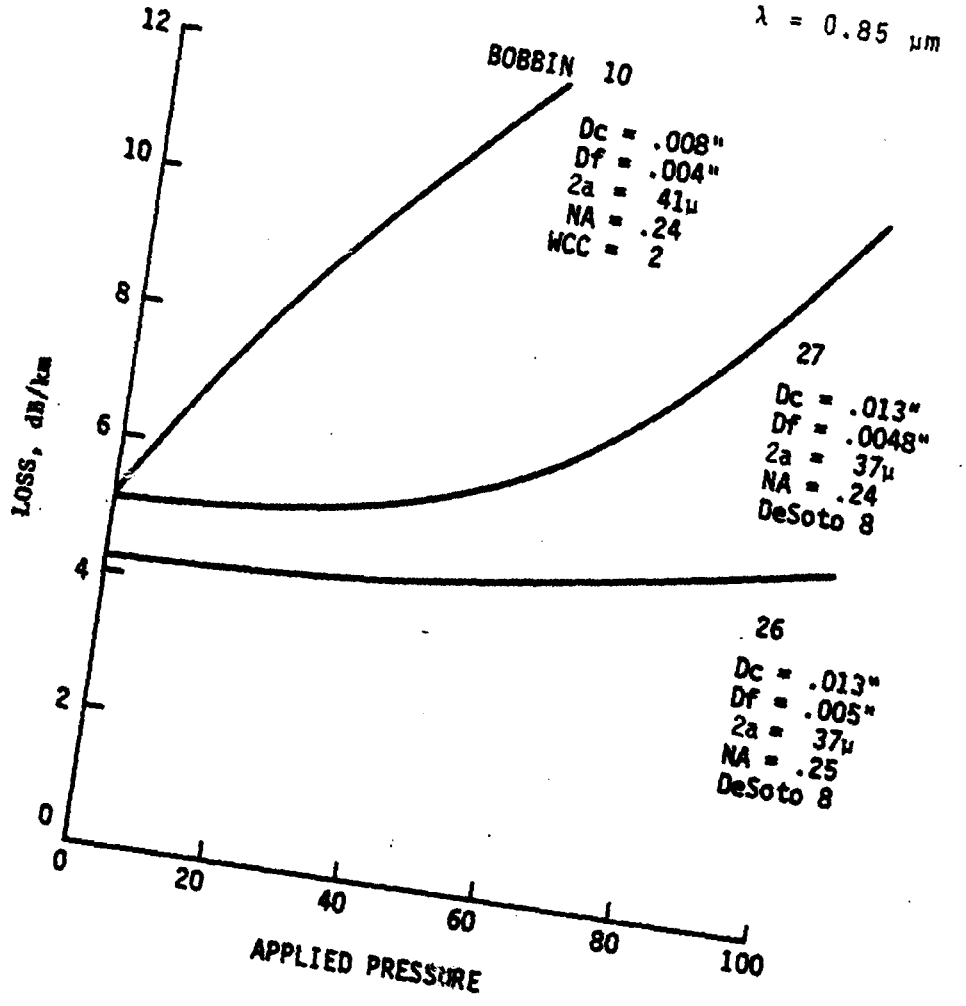

FIG. 11. ATTENUATION DATA 7.8" DIAMETER SPOOL

NOTES:

1. Dc = cable diameter
2. Df = fiber diameter
3. 2a = core diameter
4. NA = numerical aperture
5. WCC, DeSota are fiber coatings

Source: Reference 30

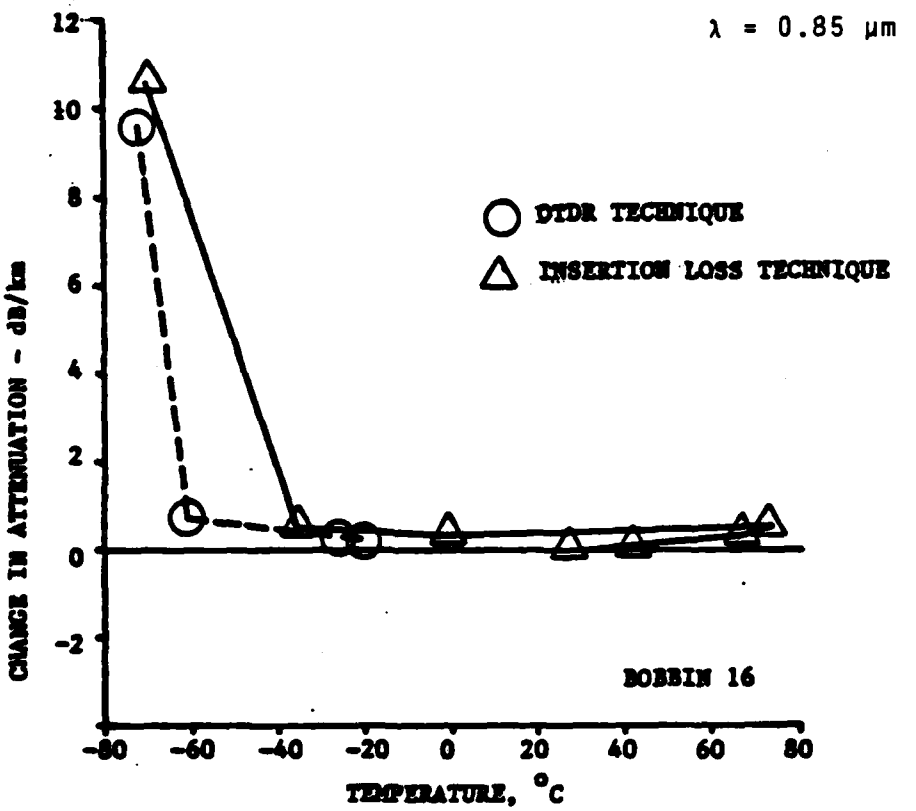

FIG. 12. EFFECT OF TEMPERATURE ON BOBBIN ATTENUATION

Source: Reference 30

3.3 OPTICAL RECEIVER CHARACTERISTICS AT 0.85 μm AND 1.3 μm

As may be observed from the intrinsic losses displayed in Figure 10, fiber optic link operation at longer wavelengths decreases these losses. Detectors for operation in the 1.0-1.6 μm region have recently been reviewed.[31] Figure 13 depicts both theoretical curves and measured data for both avalanche photodetector (APD) and PIN-FET detector receivers operating in this range at data rates between 1-1000 Mbits/sec. It may be observed from this figure that a silicon APD is the most sensitive receiver over this range of data rates (curve a). However, the responsivity of silicon falls rapidly at wavelengths above 1.1 μm, where the optical fiber loss is lowest. Although III-V alloys (curve b) and germanium (curve c) APD receivers display good sensitivities at these longer wavelengths, they have high noise characteristics due to a high ratio of the ionization rates of electrons and holes. Several experimental points for PIN-FET receivers fabricated using III-V alloys are displayed, indicating the sensitivities of these receivers are almost as high as for the longer-wavelength APD receivers. The only caution in using these receivers below 45 Mb/s is the 1/f noise commonly found in GaAs FETs. However, the data rates required in the fiber optic link missile guidance system are above this level, making their use satisfactory.

3.4 DATA RATE-LENGTH PRODUCTS FOR MULTIMODE AND SINGLE-MODE FIBER OPTIC LINKS

An estimate of the data rate-length products for both multimode and single-mode fiber optic links may be made by combining the dispersion and loss characteristics of these fibers described in Sections 3.2 and 3.3 with the receiver sensitivities of Figure 13 for a silicon APD, assuming the link operates at a wavelength of 0.85 μm using a GaAℓAs laser as the airborne unit source (as in the IFOCL and FOG-M programs).

An estimate of the total power available in the link for a power P_L launched by the laser into the fiber may be obtained by approximating Curve a in Figure 13 by the function

$$F(T) = 72 - 4.35 \ln (T^{-1}) + P_L \text{ dBm} \quad \text{(where } T^{-1} \text{ is the data rate).} \tag{14}$$

The available power is used to provide fiber and coupling loss and the ISI

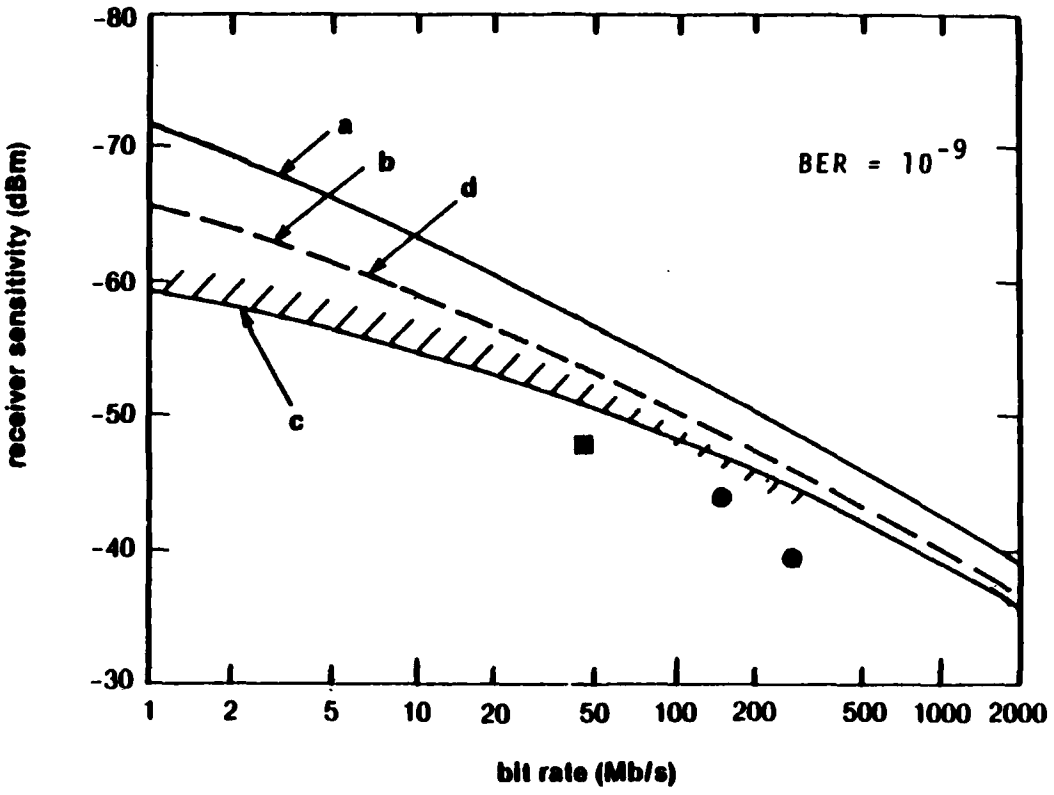

A. Si APD @ .83μm, B. III-V APD @ 1.3μm with k = 0.3, C. Ge APD WITH I_b 100 nA, III-V PIN/FET @ 1.3μm. EXPERIMENTAL RESULTS: • BPO, ■ BELL LABS,

FIG. 13. CALCULATED RECEIVER SENSITIVITIES OVER THE 1000 MB/S RANGE FOR RECEIVERS WITH A RANGE OF DETECTOR TYPES

Source: Reference 31

penalty. It may also be used to include a power margin, M, to account for additional losses due to temperature effects, receiver equalization, bias and dynamic range requirements, etc.[22]

In designing the link, the objective is to maximize the amount of information transmitted over the link for a specific link length. This corresponds to maximizing the product of data rate, T^{-1}, and the link length, L, namely, the factor L/T.

In the multimode fiber, mode dispersion dominates the total dispersion, and b takes the value 1/2, assuming the fiber is well mode mixed due to the index grading and microbending effects. For the single-mode fiber, $\psi \sim 0$ and no fiber bandwidth limit exists for data rates in the range of interest (1-1000 Mb/s). These two cases have been plotted for several cases:

1. Material dispersion is characterized by $\phi\Delta\lambda = 3 \times 10^{-10}$ sec/km.
2. Modal dispersion is characterized by two cases: $\psi = 10^{-9}$ sec/km$^{\frac{1}{2}}$ and $\psi = 3 \times 10^{-9}$ sec/km$^{\frac{1}{2}}$.
3. Total loss/km = 4.5 dB/km.
4. Link margin M = 5 dB.

These cases have been plotted in Figure 14, showing L/T vs. 1/T for data rates between 10 and 1000 MB/sec assuming P_L = 0 dBm, a typical power launched into the fiber by a laser. Note the onset of bandwidth limitation due to modal dispersion is clearly visiable. For the case $\psi = 3 \times 10^{-9}$ sec/km$^{\frac{1}{2}}$, a maximum transmission capacity is visible, the exact position of the maximum depending upon the relative interplay between fiber loss and dispersion. The fiber used in the link should be selected to obtain this maximum data rate-length capability.

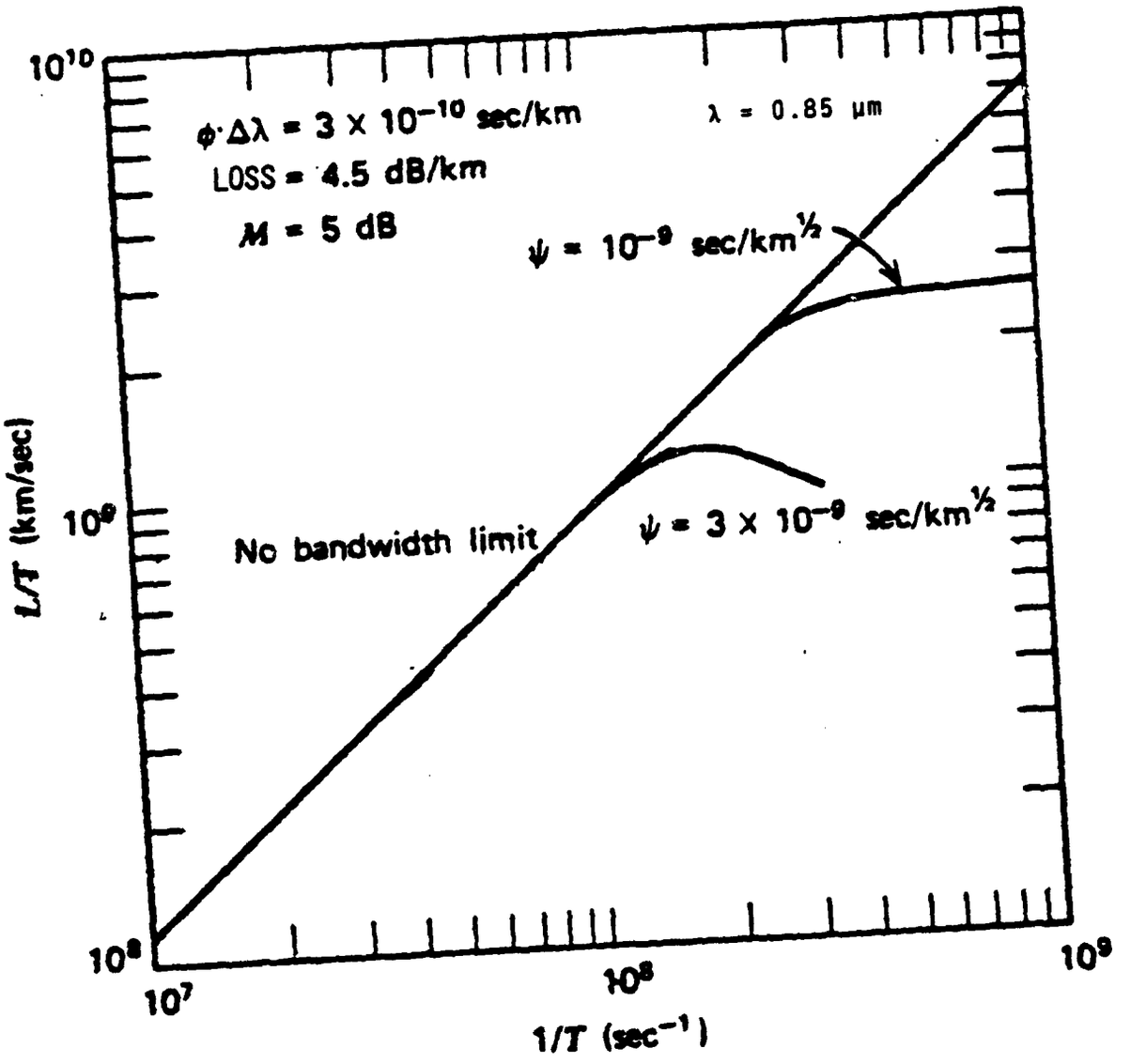

FIG.14. DATA RATE – LENGTH PRODUCTS FOR MULTIMODE OPTICAL FIBER

3.5 OPTICAL SOURCE POWER REQUIREMENTS AT 0.85 μm AND 1.3 μm FOR IFOCL AND FOG-M SYSTEMS

As calculated in Section 2.3, the data rate required to transmit a television image over a fiber optic link with a SNR of 30 dB using PFM and a negligible ISI loss penalty is approximately 8 times the television signal bandwidth. Since the IFOCL and FOG-M systems employ a 5 MHz and a 10 MHz bandwidth television signal, respectively, the required data rates are 40 and 80 MB/s.

In multimode fiber, where modal dispersion dominates, the effect of increasing optical source wavelength is primarily that of reducing Rayleigh scattering loss in the fiber, thus increasing link range when using a 1.3 μm laser. At shorter ranges, this reduced scattering loss at 1.3 μm could be used to replace the laser with an LED, thereby reducing the transmitter cost and increasing the reliability by eliminating the large temperature threshold dependence of long wavelength lasers.[32]

In order to calculate the fiber optic link source power requirements for the IFOCL and FOG-M systems, it is first necessary to determine the receiver noise equivalent power (NEP) at 0.85 μm and 1.3 μm for data rates of 40 MB/s and 80 MB/s. The NEP of a receiver is the rms value of optical power which is required to produce unity rms SNR.[33] The receiver sensitivities presented in Figure 13 assume a pulse bit error rate (BER) of 10^{-9} requiring an electrical peak pulse-to-noise ratio of 21.5 dB.[17] Assuming a square-law optical detector, this converts to 12.75 dB for an rms pulse-to-noise ratio. The receiver NEP in Table IV has been calculated from the curve in Figure 13 for the Si APD receiver (at 0.85 μm) and the experimental points for the PIN-FET (at 1.3 μm) at 40 and 80 MB/s, respectively.

The $(C/N)_i$ to achieve the electrical FM threshold of 15 dB shown in Figure 5 is also divided in half to obtain the threshold required at the receiver input. The required fiber output power is the difference between the receiver NEP and the optical $(C/N)_i$ threshold for each receiver type and data rate.

TABLE IV

FIBER OPTIC LINK SOURCE POWER REQUIREMENTS

	BIT RATE (MB/s)			
	40 (IFOCL)		80 (FOG-M)	
OPERATING WAVELENGTH (μm)	0.85	1.3	0.85	1.3
RECEIVER NEP (dBm) (at BER=10^{-9}, $(C/N)_i$ = 12.75 dBm)	-70.0	-60.0	-67.0	-57.0
$(C/N)_i$ FM THRESHOLD (dB) (referred to optical power at receiver input)	7.5	7.5	7.5	7.5
REQUIRED FIBER OUTPUT POWER (dBm)	-62.5	-52.5	-59.5	-49.5
FIBER LOSSES (10 km)				
Rayleigh Scattering (dB)	38.0	11.0	38.0	11.0
Microbending Loss (dB)	15.0	15.0	15.0	15.0
ISI Penalty (dB)	0.1	0.1	0.5	0.5
TOTAL (dB)	53.1	26.1	53.5	26.5
COUPLER LOSSES (dB)	4.0	4.0	4.0	4.0
SPLICE AND CONNECTOR LOSSES (dB)	3.0	3.0	3.0	3.0
TOTAL LINK LOSSES	60.1	33.1	60.5	33.5
OPERATING MARGIN(Temp.,Bias,etc.)(dB)	5.0	5.0	5.0	5.0
TOTAL LINK LOSSES (dB)	65.1	38.1	65.5	38.5
MINIMUM OPTICAL SOURCE POWER COUPLED INTO THE FIBER (dBm)	2.6	-14.4	6.0	-11.0

Intrinsic fiber losses at 0.85 μm and 1.3 μm, based upon measurements made by ITT/EOPD,[34] are listed in Table V. The total losses for a 10 kilometer length of fiber operating at 0.85 μm and 1.3 μm are the same for both the IFOCL and FOG-M systems in Table IV, since this loss is independent of data rate.

Microbending loss measured for 37 μm -core optical fiber of the type which might be used in these demonstrations is given in Figure 11. It was shown in Reference 30 that the microbending loss for this fiber type is independent of wavelength and data rate. It is anticipated that a lower microbending-loss fiber will be developed for the IFOCL and FOG-M programs. Therefore, a microbending loss of 1.5 dB/km has been assumed for all the cases considered in Table IV.

The ISI penalty increases with data rate (1/T) for a particular value of τ_e, as displayed in Figure 6. The value of τ_e increases with fiber material and modal dispersion according to Eq.(8). Therefore, it is assumed that an optical fiber is used which will keep the ratio $(\tau_e/T) \leq 0.5$ at a data rate of 40 Mb/s, resulting in an ISI loss penalty of 0.1 dB at a data rate of 40 Mb/s.

TABLE V

35-μm MISSILE FIBER RAYLEIGH SCATTERING LOSS

FIBER 811027-13C
3580 METERS

WAVELENGTH (μm)	LOSS (dB/km)
0.85	3.83
1.05	2.07
1.30	1.13
1.54	1.07

Source: ITT/EOPD (Ref.34)

Bidirectional coupler loss has been measured at 2 dB,[34] resulting in a total of 4 dB for the two couplers in Figure 1. Splice and connector losses for the 35 μm fiber have been measured at a total of 3 dB for the link.[34] All these losses are practically independent of wavelength and data rate.

Adding a 5 dB operating margin for the effects of temperature, bias, dynamic range, etc., the total link losses for each case are tabulated in Table IV. Taking the difference between these losses and the required fiber output power yields the minimum optical source power for each case, listed at the bottom of Table IV. Note that the minimum optical power required to be coupled into the fiber is 17 dB larger for the system operating at 0.85 μm than for the 1.3 μm system. The power levels needed at the 0.85 μm wavelength require a laser, while the coupled source power required for the link operating at 1.3 μm could be supplied by an edge-emitting LED.[35] Longer ranges than 10 kilometers would be achieved using a laser operating at 1.3 μm.

3.6 TEMPERATURE, COUPLING, AND FREQUENCY RESPONSE CHARACTERISTICS OF OPTICAL SOURCES

The temperature sensitivity of a laser may be determined by examining the threshold current, I_{th}, required for the onset of lasing.[35] A calculated curve and measured values for the threshold variation with temperature of a laser operating at 1.25 μm are displayed in Figure 15. Note that the increase in threshold current varies exponentially with temperature. Therefore an expression which is used to predict the

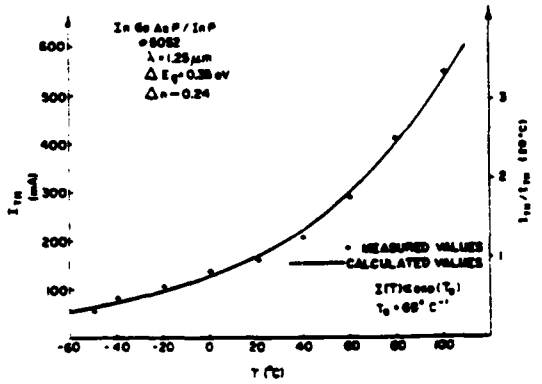

FIG. 15 TEMPERATURE DEPENDENCE OF PULSED THRESHOLD CURRENT FOR AN InGaAsP LASER DIODE

Source: Reference 32

increase in I_{th} with temperature is:[32]

$$I_{th} \propto \exp. \left(\frac{\Delta T}{T_o}\right) , \tag{15}$$

where

ΔT = change in junction temperature (°C)

T_o = threshold temperature (°C)

Values of T_o for AℓGaAs and InGaAsP laser diodes operating at the 0.85μm and 1.3μm wavelengths are given in Table VI along with the spectral shifts due to changes in operating temperature.

TABLE VI

LASER TEMPERATURE CHARACTERISTICS

	T_o(*)(°C)	Spectral Shift With Operating Temperature $\Delta\lambda/\Delta T$ (Å/°C)	Possible Wavelength Range λ (μm)
AℓGaAs	140 - 190	2 - 3	0.7 - 0.9
InGaAsP	40 - 75	4 -5	1.0 - 1.7

Note that the temperature sensitivity of InGaAsP lasers are 2-3 greater than for AℓGaAs lasers. Although thermoelectric cooling is used to reduce this temperature sensitivity, they introduce a source of possible failure and turn-on time delay.

The temperature characteristics of a long wavelength LED which might be used in a link of length less than 10 kilometers are shown in Figure 16a, with the output power and power coupled into a 55 μm-core graded index fiber having a numerical aperture (NA) of 0.25, given in Figure 16b. Observe that the linear region of the coupled power extends to over 100 μW, suitable for the 1.3 μm IFOCL and FOG-M systems. However, the 35 μm-core fiber used in these systems would not couple enough power

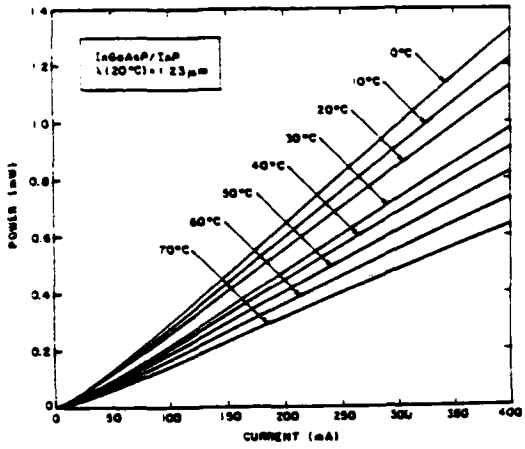

(a) LED OUTPUT POWER VS. DRIVE CURRENT AND TEMPERATURE.

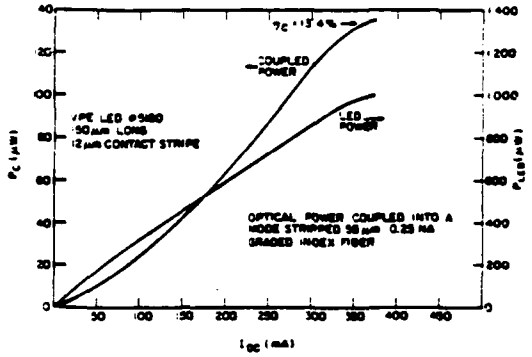

(b) InGaAsP LED OUTPUT POWER (total and fiber-coupled) VS. DRIVE CURRENT.

FIG.16. LONG WAVELENGTH LED CHARACTERISTICS

Source: Reference 32

from a surface-emitting LED, and therefore an edge-emitting LED or a laser would be required to supply the power required for a 10 kilometer link.

Edge-emitting LEDS are capable of coupling 5-6 times the power into a low NA fiber as surface-emitting LEDs.[36] A comparison of optical power coupled into optical fibers of different NAs from surface- and edge-emitting LEDs are shown in Figure 17. Note that considerably more power is coupled into optical fibers with NAs less than 0.3 by edge-emitting LEDs and that above this value, the surface-emitting diode couples power more efficiently. This is due to the more focused beam of an edge-emitting LED.

Another advantage of edge-emitting LEDs is their improved frequency response, as shown in Figure 18. This is because the frequency response improvement of a surface-emitting LED requires heavy active layer doping, thus reducing the output power while an edge-emitting LED's active layer is virtually undoped. Lasers have frequency responses above 1 GHz.[35]

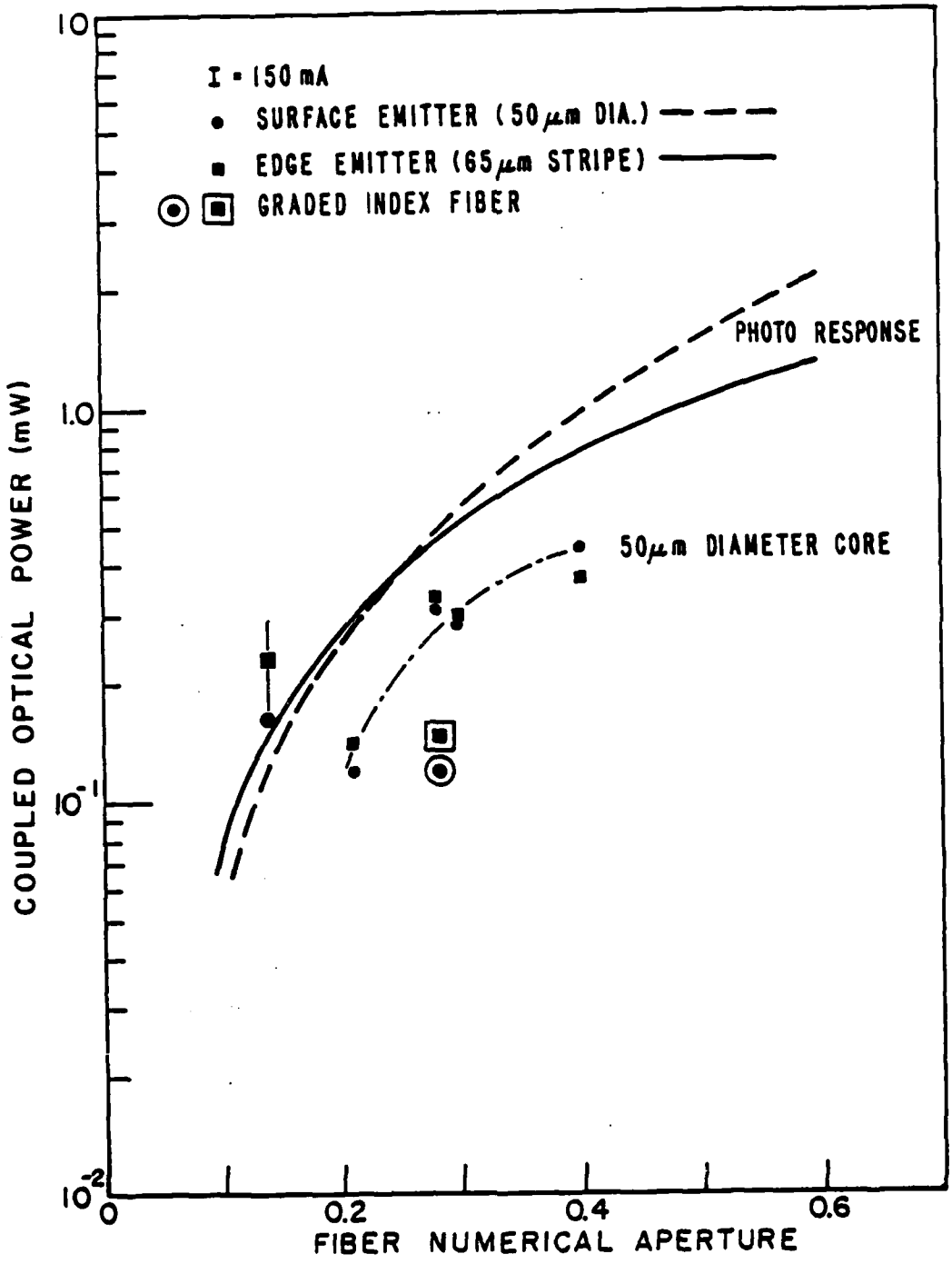

FIG. 17. COUPLED OPTICAL POWER VS. FIBER NA FOR TYPICAL SURFACE- AND EDGE-EMITTINGS LEDs

SOURCE: Reference 36

Source: Reference 36

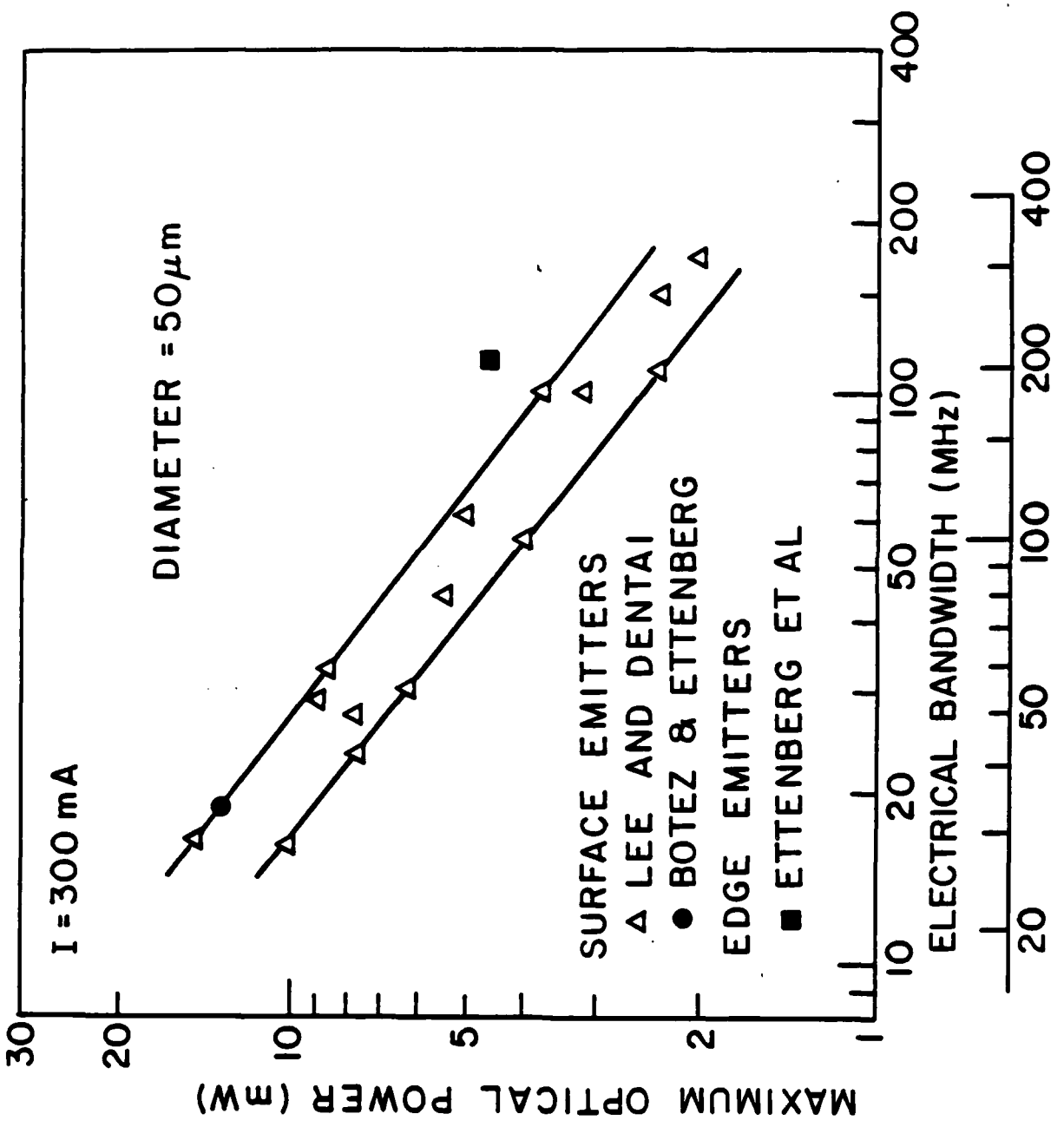

FIG. 18. OUTPUT OPTICAL POWER AT VS. BANDWIDTH FOR SURFACE- AND EDGE-EMITTING LEDs

4.0 SPOOLING LOSS IN THE FIBER OPTIC LINK

As discussed in Sections 3.3 and 3.5, microbending loss is a very important consideration in determining the range of a fiber optic link used for missile guidance. A careful analysis of the considerations involved in the optimization of the optical fiber used as a data link for missile guidance has been presented with experimental results describing the effects of fiber core diameter on spooling and coupling losses.[20] It was shown in this reference that both the source coupling efficiency and the bidirectional coupler losses are essentially independent of core diameter; therefore, the preferred design is driven by spooling loss.

Spooling loss in the fiber optic link is due to microbending caused by the precision-winding on a tapered aluminum spool of multiple layers of the fiber.[20] Each layer forms a helix, with successive layers of the fiber nesting in the grooves of the previous layer. These grooves form a helix which propagates in the direction opposite to that of the previous layer. Fiber crossovers are necessary in order to insure that all layers propagate in the same direction in order to minimize the torque on the fiber as it pays out. The number of crossovers is approximately twice the number of layers. Each crossover produces a microbending effect in the fiber, which causes the spooling loss.

4.1 MICROBENDING LOSSES IN MULTIMODE AND SINGLE-MODE OPTICAL FIBERS

A qualitative analysis of the microbending loss in graded-index multimode optical fibers relating the random bends in the fiber to its mechanical properties and coupling between the propagating and radiation (loss) modes shows that this loss is proportional to the square of the core diameter and inversely proportional to the sixth power of outer fiber diameter and the cube of the index of refraction difference between the core and cladding.[37] Measurements of spooling loss presented in Reference 20 indicate that this loss is a quadratic function of core diameter, as predicted in a more recent paper.[38] In general, microbending loss in multimode graded-index fiber is proportional to $\frac{1}{\Delta}(\frac{a^2}{\Delta})^P$, where P is a measure of the curvature power spectrum (equal to 2 for large mode mixing due to microbending effects).[39]

A reduction in the microbending loss of multimode fiber has been predicted,[40] and observed,[41] through the use of a double-cladding (W-type) structure. In this type of fiber an inner cladding refractive index, lower than the outer cladding index, is used to improve the confinement of propagating modes in order to minimize radiation loss due to microbending effects. It has also been shown that the double cladding improves the transmission bandwidth of the fiber.[40] The same type of structure has recently been employed to reduce microbending loss in single-mode fiber,[42-44] which exhibits very large microbending loss in the single-clad structure.[45] This depressed-index cladding single-mode optical fiber, developed for use in the BELL System submarine cable,[46] has tensile proof test strength of greater than 200,000 psi. It, therefore, is an excellent candidate for use in the fiber optic guidance link when very high data-rates and over long ranges are required.

The depressed-index cladding single-mode fiber typically has a germania-silicate deposited core with a relative refractive index above silica. Flourine is deposited within an inner cladding to depress its refractive index below that of a pure silica outer cladding. Microbending losses are low below a loss edge, determined by the wavelength at which the mode effective index falls below the index of the substrate tube.[43] If the system operating wavelength is kept below this loss edge, control is maintained by keeping the depressed-index cladding width large compared with the core diameter (ratio > 7).[44] Although the loss edge wavelength decreases with microbending, the loss edge wavelengths can be kept larger than 2.0 μm for these large ratios, thus controlling microbending losses. Thus, the system may be operated at the zero-dispersion wavelength of 1.3 μm while minimizing microbending losses.

4.2 BANDWIDTH INCREASE IN MULTIMODE OPTICAL FIBERS RESULTING FROM MODE COUPLING DUE TO MICROBENDING EFFECTS

Although microbending effects in multimode fiber introduce loss, they concurrently increase the effective bandwidth of the fiber, which could be used to increase the link capacity by increasing the SNR using a modulation technique such as PFM, as discussed in Section 2.3. This bandwidth increase with loss, such as that introduced by an increase in

mode coupling due to microbending effects, may be observed by examining the decrease in rms pulse width, σ , as the loss is increased from 2dB/km to 10 dB/km due to mode coupling, as may be seen in Figure 19. This effect has been shown to follow the relationship as a function of grading index α , shown plotted in Figure 20:[47]

$$R^2\beta = 4.3\gamma L_c \tag{16}$$

where

$$R = \frac{\sigma \text{ (coupled)}}{\sigma \text{ (uncoupled)}}$$

β = loss penalty due to mode coupling (dB)

γ = intrinsic loss of fiber (dB)

L_c = coupling length

Observe from Figure 20 that for a particular index grading profile the $R^2\beta$ product is a constant. Therefore, since the fiber bandwidth is inversely proportional to rms pulse width σ, the ratio of bandwidth increase resulting from mode coupling due to microbending effects may be expressed as:

$$\frac{B_1}{B_o} = \sqrt{\frac{\beta_1}{\beta_o}} \tag{17}$$

where

B_o = initial bandwidth before spooling

B_1 = bandwidth after spooling

$\beta_o = \gamma$ = intrinsic loss (dB)

β_1 = loss penalty due to mode coupling caused by microbending (dB)

An experimental verification of this relationship is shown in Figure 21. Note that the output pulse shown in Figure 21b from a 155 meter graded-index ITT/EOPD multimode fiber is attenuated and spread compared to the input pulse of Figure 21a. When placed under pressure on a spool, the loss increases 4.5 dB, but the rms pulse width has decreased by a factor of 2.12, thus increasing the fiber bandwidth by this amount, as demonstrated in Figure 21c. These measurements confirm the relationship between bandwidth increase and spooling loss given in Eq.(17).

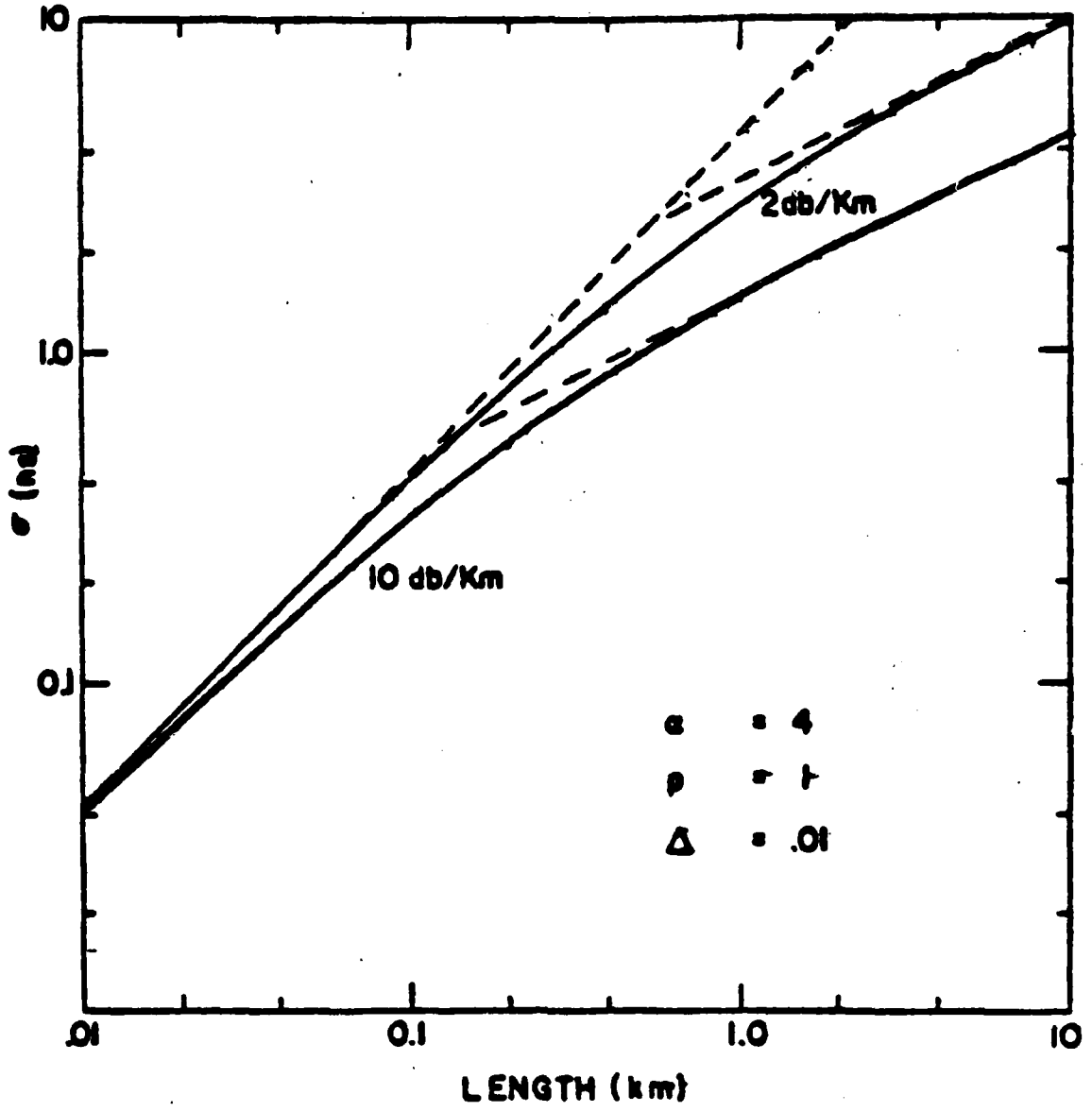

FIG. 19. RMS PULSE WIDTH VS. LENGTH MODE COUPLING

Source: Reference 47

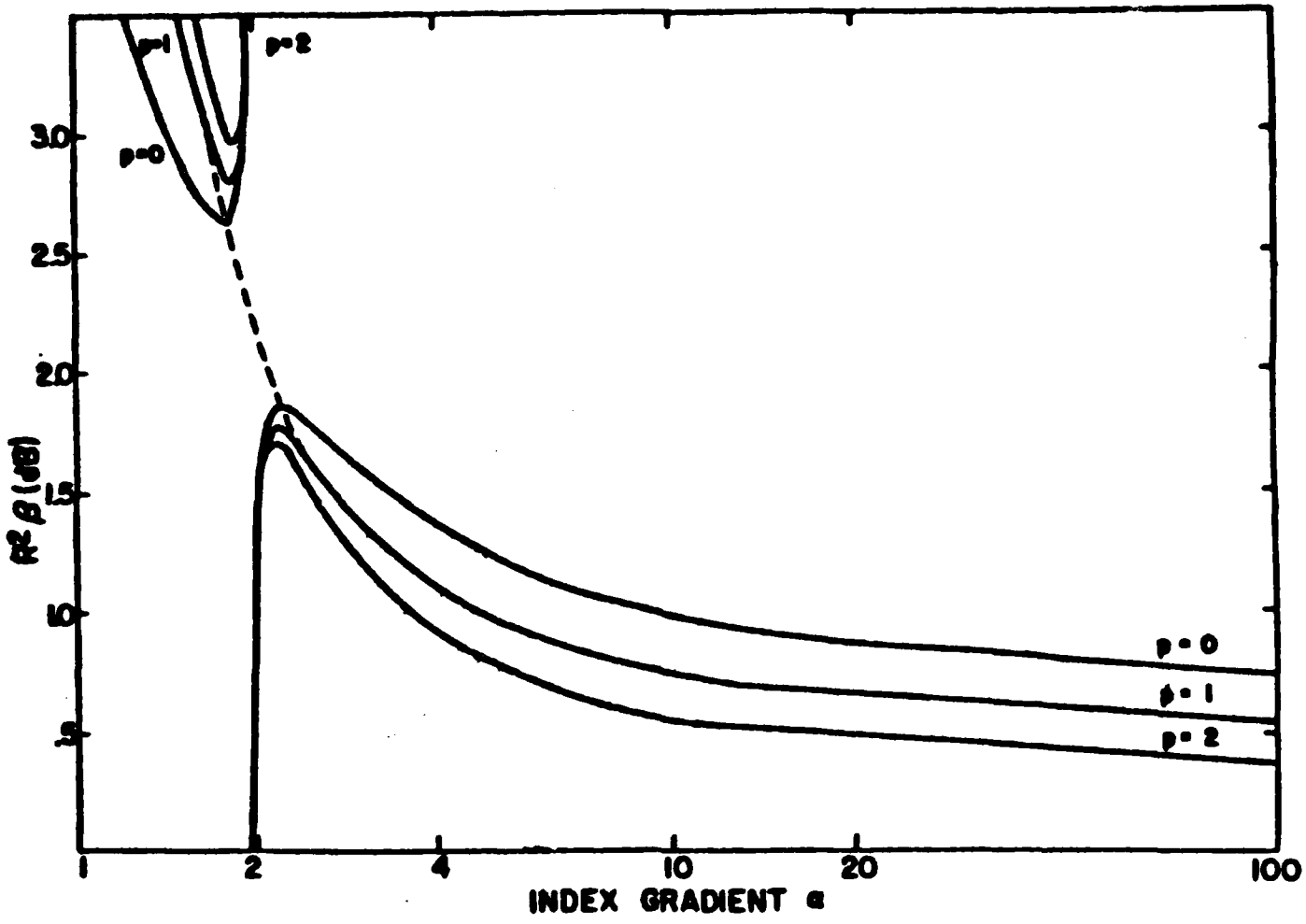

FIG. 20. RELATIONSHIP BETWEEN DECREASE IN RMS PULSE WIDTH AND LOSS PENALTY

Source: Reference 47

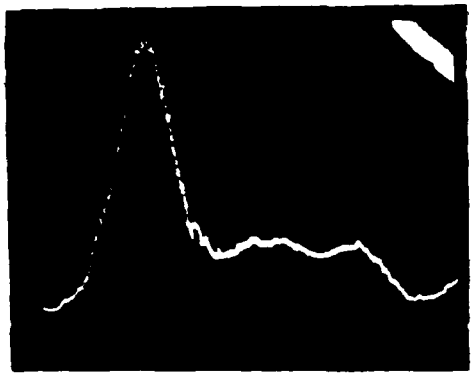

INPUT PULSE
100PS/DIV, 50 MV/DIV
3 dB PULSE WIDTH = 160 PS

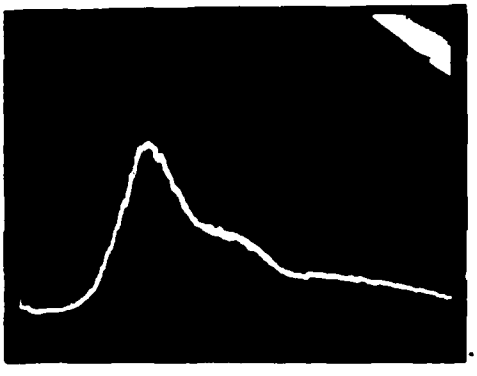

OUTPUT PULSE FROM 155 METER
G.I. FIBER
200 PS/DIV , 50 MV/DIV
3 dB PULSE WIDTH = 360 PS
RELATIVE AREA UNDER CURVE =
1.20×10^5 (MV)(PS)

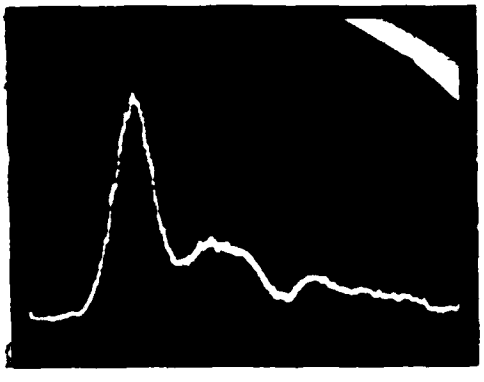

OUTPUT PULSE FROM THE SAME FIBER
UNDER PRESSURE
200 PS/DIV, 20 MV/DIV
3 dB PULSE WIDTH = 220 PS/DIV
RELATIVE AREA UNDER CURVE =
4.2×10^4 (MV)(PS)

LOSS = 4.5 dB

$$\frac{B_1}{B_o} = \frac{R_o}{R_1} = 2.12$$

5.0 OPTICAL MULTIPLEXING FOR INCREASED FIBER OPTIC LINK INFORMATION CAPACITY

Further information capacity increase may be achieved through the use of optical multiplexing techniques.[35] For example, wavelength-division multiplexing (WDM) may be used to add additional channels to the bidirectional fiber optic link by providing an additional channel in each direction. This would enable the transmission of both television and I.R. image signals over the same fiber simultaneously without loss in data rate of either signal. This would require, however, the use of a separate optical source and receiver for each channel.

In WDM technology, optical multi/demultiplexers are used to separate the wavelength of each channel. This may be achieved through the use of a variety of optical techniques such as interference filters, diffraction gratings, or prisms.[35] Although interference filters are currently being employed to achieve the wavelength selection, the highest wavelength resolution is achievable with diffraction gratings. High resolution is required to obtain the maximum number of channels with minimum interference.

Another consideration in the design of a WDM system is crosstalk between channels. The isolation between bidirectional digital video channels is about 30 dB, while multiplexed channels transmitting information in the same direction require twice this amount of isolation. This is due to reflection and scattering from the connectors and fiber, causing interference at the receiver to be isolated from transmitters at the same side of the link. A particularly effective WDM multi/demultiplexer which provides this level of isolation between channels uses both interference and grating filters, is illustrated in Figure 22.[48] Note the large separation between channels transmitting light in opposite directions (1,2 and 3,4). The optical sources used in a WDM must also have good wavelength stability. As discussed in Section 3.5, long-wavelength lasers would have to be stabilized with a thermoelectric cooler for this application.

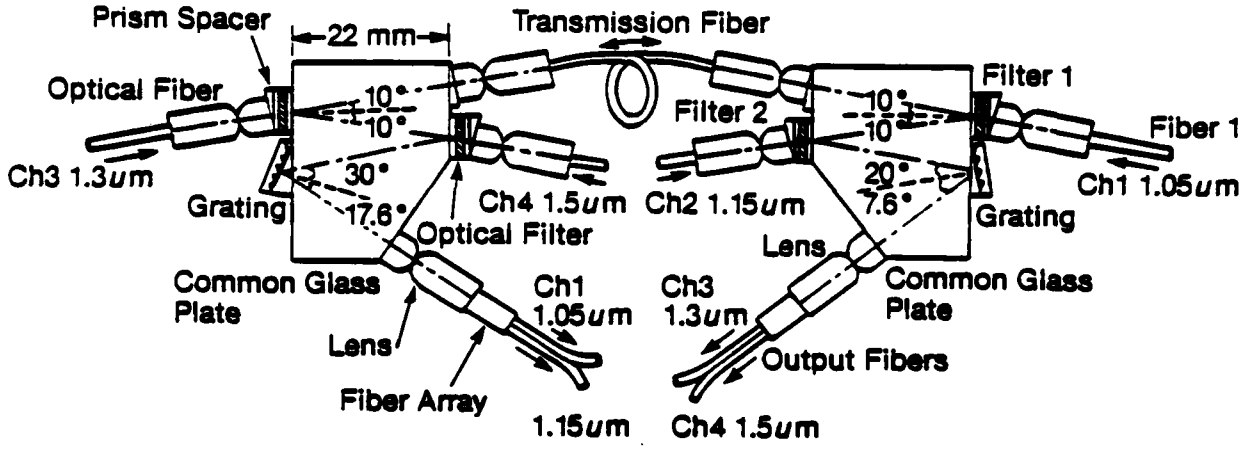

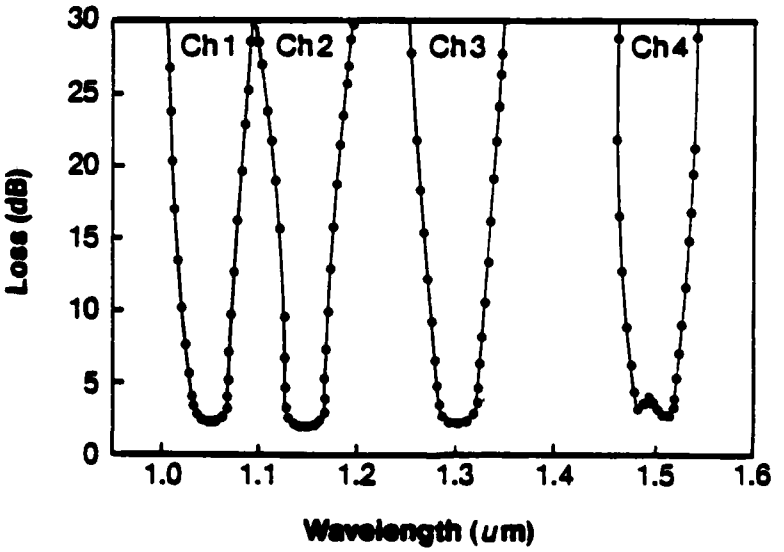

FIG. 22. WAVELENGTH SELECTIVITY USING INTERFERENCE AND GRATING FILTERS

Source: Reference 48

6.0 CONCLUSIONS AND RECOMMENDATIONS

The conclusions which may be drawn from this study are:

1. The currently graded index multimode optical fiber exhibits excess data rate capability which may be used to increase the SNR of video signals or to transmit coded I.R. seeker signals.

2. Although spooling loss is an important factor, the IFOCL and FOG-M system ranges are limited primarily by Rayleigh scattering losses at 0.85 μm. Increased range may be achieved by use of 1.3 μm lasers, or edge-emitting LEDs could be used to achieve 10 km range with 35 μm-core optical fiber at reduced cost and increased reliability.

3. Currently available 1.3 μm lasers are highly temperature sensitive, and therefore require thermoelectric cooling and power stabilization circuits.

4. Smaller core diameter optical fiber is required to further reduce spooling (microbending) loss to achieve an extended system range.

5. Higher data rates are available with multimode optical fiber as a result of the increased bandwidth due to mode coupling caused by microbending effects.

6. High-strength single-mode optical fiber is becoming available and may be used to further increase data rate.

7. Optical multiplexing techniques may be used to further increase optical fiber capacity.

The following recommendations are made for an enhanced optical fiber guidance system communication link:

1. Reduce multimode optical fiber core size to decrease spooling (microbending) loss.

2. Determine the minimum multimode fiber core size before light deconfinement effects due to microbending (as calculated for single-mode fibers) begin to increase losses.

3. Confirm single-mode and low-mode optical fiber microbending loss effects by measurements.

4. Increase laser wavelength to 1.3 μm to reduce Rayleigh scattering loss.

5. Reduce temperature sensitivity of 1.3 μm threshold by developing improved materials and structures.

6. Examine the possibility of using edge-emitting 1.3 μm LED sources to reduce the temperature sensitivity and cost.

7. Examine the use of other modulation techniques, e.g., PCM.

8. Study the distortion effects on image quality as a function of fiber optic system data rate for specific modulation techniques.

7.0 ACKNOWLEDGMENTS

The work contained in this report is the product of the efforts of a number of individuals who provided significantly to the information and evaluation of the results. I am particularly indebted to Mr. Ray Farmer, who, in his capacity as COTR, provided the guidance and support required at the appropriate times throughout this program. I also wish to thank Dr. William Pittman for his confidence and encouragement in this effort. Extremely valuable technical information about the FOG programs was provided by Messrs. Rex Powell, Paul Jacobs, and R.M. Autery of the Missile Laboratory, and I owe particular gratitude for the time devoted to this project by Dr. Howard Wichansky of CECOM. Messrs. Dave Fox and Steve Anderson of Hughes Aircraft have been extremely helpful in providing much of the information on the spooling characteristics of the fiber. The information supplied by Messrs. Ken Ferris, George Gasparian, and Willis Muska of ITT/EOPD, were major contributions to my understanding of the modulation, electronics, optical sources, detectors, and couplers used in the systems described in this report. As usual, the typing was performed efficiently and professionally by Mrs. Kae Wilkens.

8.0 REFERENCES

1. Powell, R.B., "Development of Optical Fiber Data Link for Missile Guidance," Letter Report RD-82-1 DRSMI-RDD, December 1981.

2. Wichansky, H., "Fiber Optics Team Multichannel Transmission Division CECOMS," Trip Report DRSEL-COM-RM-1, April 1982.

3. Discussions with Hughes Aircraft Personnel, Canoga Park, CA.

4. Wichansky, H., Powell, R.B., and Fox, D., "Fiber Optic Implications for Missile Guidance Design," presented at ELECTRO '81 Professional Program, April 1981.

5. Budrikis, Z.L., "Visual Fidelity Criterion and Modeling," *Proceedings IEEE*, Vol.60, No.7, pp.771-779, July 1972.

6. "Application of Operator Video Bandwidth Compression/Reduction Research to RPV System Design," prepared by Hughes Aircraft for ERADCOM, August 1981

7. Shannon, C.E., "A Mathematical Theory of Communication," *Bell Syst. Tech. Journal*, Vol.27, pp.379-623, 1948.

8. Shannon, C.E., "Coding Theorem for a Discrete Source with a Fidelity Criterion," in *Information and Decision Procedures*, R.E. Machol, Ed., McGraw-Hill, 1960.

9. Kolmogorov, A.N., "On the Shannon Theory of Information Transmission of Continuous Signals," *IRE Trans. Inform. Theory*, Vol. IT-2, pp.401-407, May 1969.

10. McDonald, R.A. and Schultheiss, P.M., "Information Rates of Gaussian Signals Under Criteria Constraining the Error Spectrum" *Proc. IEEE*, Vol.52, pp.415-416, April 1964.

11. Hayes, J.F., Habibi, A., and Wintz, P.A., "Rate Distortion Function for a Gaussian Source Model of Images," *IEEE Trans. Inform. Theory*, Vol. IT-16, pp.507-508, July 1970.

12. Tasto, M. and Wintz, P.A., "A Bound on the Rate-Distortion Function and Application to Images," *IEEE Trans. Inform. Theory*, Vol. IT-18, pp.150-159, January 1972.

13. Netravali, A.N. and Limb, J.O., "Picture Coding: A Review," *Proc. IEEE*, Vol.68, No.3, pp.367-406, March 1980.

14. Members of the Technical Staff, Bell Telephone Laboratories, *Transmission Systems for Communications*, Revised Fourth Edition, December 1971, pp.693-707.

15. Fink, D.G, *Television Engineering Handbook*, McGraw-Hill, NY, 1957.

16. Electronic Industries Association Standard 170.

17. Haykin, S., *Communication Systems*, John Wiley & Sons, Inc., NY, 1978.

18. Timmermann, C., "Signal-to-Noise Ratio of a Video Signal Transmitted by a Fiber-Optic System Using Pulse-Frequency Modulation," *IEEE Trans. on Broadcasting*, Vol.BC-23, No.1, pp.12-16, March 1977.

19. Cowen, S.J., "Fiber Optic Video Transmission System Employing Pulse Frequency Modulation," *Proc. of Oceans*, pp.253-259, September 1979.

20. Fox, D.S., Akers, F., and Gasparian, G., "Optimization of an Optical Fiber for Missile Guidance Applications," *Proceedings of SPIE Conf.*, San Diego, August 1981.

21. Taub, H. and Schilling, D., *Principles of Communication Systems*, Mc-Graw Hill, NY, 1971.

22. Midwinter, J.E., *Optical Fibers For Transmission*, John Wiley & Sons, Inc., NY, 1979.

23. Fleming, J.W., "Material Dispersion in Lightguide Glass," *Electron. Lett.*, Vol.14, 11, pp.324-326, May 1978.

24. Yamada, J., et.al., "High Speed Optical Pulse Transmission at 1.29 μm Wavelength Using Low-Loss Single-Mode Fibers," *IEEE J. Quntum Elec.*, Vol. QE-14, pp.791-800, November 1978.

25. Masterson, J.B. and Peveler, J., "Up-date on the Performance of Field Installed Optic Cables," *Proc. 28th Int. Wire and Cable Symposium*, pp.364-369, Cherry Hill, NJ, 1979.

26. Kaminow, J., Marcuse, D., and Presby, H., "Multimode Fiber Bandwidth: Theory and Practice," *Proc. IEEE*, Vol.68, 10, pp.1209-1213, October 1980.

27. Love, W.F., "Statistical Time Delay Equalization in Multimode Optical Fibers," *Tech. Dig. of Topical Meeting on Opt. Fiber Comm.*, p.27, Phoenix, April 1982.

28. Chapman, J. and Slaughter, R., "Bandwidth Enhancement in Optical Cable Installations," Paper WAA1, *ibid.*

29. Muja, T, et.al., "Ultimate Low-Loss Single-Mode Fiber at 1.55 μm," *Electron. Lett.*, Vol.15, pp.106-108, February 15, 1979.

30. Fox, D. and Glavas, X., "High Strength Rapid Payout Fiber Optic Cable Assembly," CORADCOM Tech. Report 78-2964-F, April 1981.

31. Conradi, J., "Detectors for Fiber Optical Communications in the 1.0-1.6 μm Region," *Proc. SPIE Conference*, Vol.266, pp.49-55, Los Angeles, February 1981.

32. Channin, D. and Ettenberg, M., "InGaAsP Sources and Detectors for the 1.0-1.7 μm Wavelength Range," *ibid,* pp.40-48.

33. Gallawa, R., "A Users Manual for Optical Waveguide Communications," U.S. Army Communications Command, Ft. Huachuca, AZ, March 1976.

34. Ferris, K., Gasparian, G., and Muska, W., "Fiber Optic Communication System for Missile Guidance Final Technical Report," prepared for the U.S. Army Missile Command, June 15, 1981.

35. Botez, D. and Herskowitz, G.J., "New Developments in Components for Optical Communications - A Review," *Proc. IEEE,* Vol.68, No.6, pp.689-731, June 1980.

36. Botez, D. and Ettenberg, M., "Comparison of Surface- and Edge-Emitting LEDs for Use in Fiber-Optical Communications," *IEEE Trans. Electron. Devices,* Vol. ED-26, pp.1230-1238, August 1979.

37. Olshansky, R., "Distortion Losses in Cabled Optical Fibers," *Appl. Optics,* Vol.14, No.1, pp.20-21, January 1975.

38. Seikai, S., et.al., "Optimization of Multimode Graded-Index Fiber Parameters: Design Considerations," *Appl. Optics,* Vol.19, No.16, pp.2860-2865, 15 August 1980.

39. Olshansky, R., "Propagation in Glass Optical Waveguides," *Rev. Mod. Phys.,* Vol.51, No.12, pp.343-367, April 1979.

40. Kowakamis, S., et.al., "Transmission Characteristics of W-Type Optical Fibers," *Proc. IEEE,* Vol.123, No.6, pp.5686-590, June 1976.

41. Tanaka, T., et.al., "Microbending Losses in Doubly Clad (W-Type) Optical Fibers," *Appl. Optics,* Vol.16, No.9, pp.2391-2394, September 1977.

42. Cohen, L., Marcuse, D., and Mammel,W.,"Controlling Leaky-Mode Loss and Dispersion in Single-Mode Lightguides with Depressed-Index Claddings," Tech. Digest of Topical Meeting on *Optical Fiber Comm.,* p.52, Phoenix, April 1982.

43. Lazay, P. and Pearson, A., "Control of the Long-Wavelength Loss Edge in Single-Mode Fibers with Depressed-Index Cladding," *ibid.*

44. Ainslie, B., et.al., "Transmission Properties of Depress-Cladding Monomode Fibers," *ibid.*

45. Marcuse, D., "Microbending Losses of Single-Mode, Step-Index and Multimode, Parabolic-Index Fibers," *Bell System Tech. Journal,* Vol.55, No.7, pp.937-956, September 1976.

46. Runge, P., et.al., "101-km Lightwave Undersea Experiment at 274 Mb/s," *ibid,* post-deadline paper.

47. Olshansky, R., "Mode Coupling Effects in Graded-Index Optical Fibers," *Appl. Optics*, Vol.14, No.4, pp.935-944, April 1975.

48. Watanable, R., et.al., "Optical Multi/Demultiplexers for Single-Mode Fiber Transmission," *IEEE Journal Quant. Elec.*, Vol.QE-17, No.6, pp.974-981, June 1981.